

# 4 Laboratory tests for properties of sediments in subsiding areas, by A. I. Johnson and Working Group

## 4.1 INTRODUCTION

Laboratory tests of core samples are made to determine their physical, hydrologic, and engineering properties and their consolidation and rebound characteristics. The laboratory test results then are utilized, along with the observed changes in artesian head, to compute compaction of the aquifer system on the basis of soil mechanics theory. In addition, the mineralogy and petrography of samples is determined in the laboratory in order to study these properties with special reference to the environment of deposition.

This chapter briefly describes some of the test methods used in the laboratory and presents examples of the tables and graphs summarizing the properties for compacting sediments in the specific study area--primarily the San Joaquin Valley, with some reference to the Santa Clara Valley, both in central California. The physical and geologic characteristics and the subsidence problems for these areas are described in Case Histories 9.13 and 9.14 and all laboratory methods and data are presented in more detail in the report by Johnson, Moston, and Morris (1968). The laboratory analyses that were used directly in this case study were primarily the particle-size distribution, specific gravity and unit weight, porosity and void ratio, and the consolidation and rebound tests. The tests of Atterberg limits and indices were not used quantitatively in the central California study but provided supplementary data that furnish at least a qualitative index to the compressibility characteristics of the sediments. For example, in the Unified Soil Classification system, the liquid limit is used to distinguish between clay of high compressibility and clay of low compressibility. The tests of permeability were useful in related studies. The tests comparing permeability parallel and normal to the stratification gave some data on the relative ease of movement of water in the two directions, and thus were of use in studies of leakage through confining beds.

Applications of laboratory-test data may be found in chapters 3 and 5 and in some case histories in Chapter 9 (such as 9.3, 9.13 and 9.14).

## 4.2 FIELD SAMPLING

The samples for which test results are discussed later in this chapter were obtained from core holes in the San Joaquin and Santa Clara Valleys, in Central California. Eight core holes were drilled to depths as great as 620 m and samples were collected from these core holes for analysis in the laboratory.

The core holes were drilled by a rotary-drilling rig, utilizing core barrels of the double-tube type, which have an outer rotating barrel and an inner stationary barrel. The inside diameter of the core barrel was nominally 7.6 cm and the average diameter of core recovered was about 7 cm. In most of the work, a core barrel capable of taking a core 3 m long was used. A 6-m core barrel was tried but did not give as good core recovery.

Above the Corcoran Clay Member of the Tulare Formation in the Los Banos-Kettleman City area, (Figure 4.1) a 3-m interval was cored after each 9-m of drilling. Below the top of the Corcoran Clay Member, coring was generally continuous to the bottom of the hole. Core recovery was excellent for unconsolidated to semiconsolidated alluvial deposits of sand, silt, and clay. For example, at core hole 14/13-11D1, the accumulated cored interval was 302 m and the aggregate core footage brought to land surface was 211 m, an average core recovery of 70 per cent. Core recovery was as high as 80 per cent and as low as 30 per cent. The lowest recovery was in the coarse, loose water-bearing material. Hence, the core suite obtained did not contain a representative sampling of the coarser, most permeable layers.

At each of the drilling sites, cores were laid out in sequence in 1.2-m wooden core boxes and properly labelled for future reference. From each 3-m interval cored, the following samples were collected:

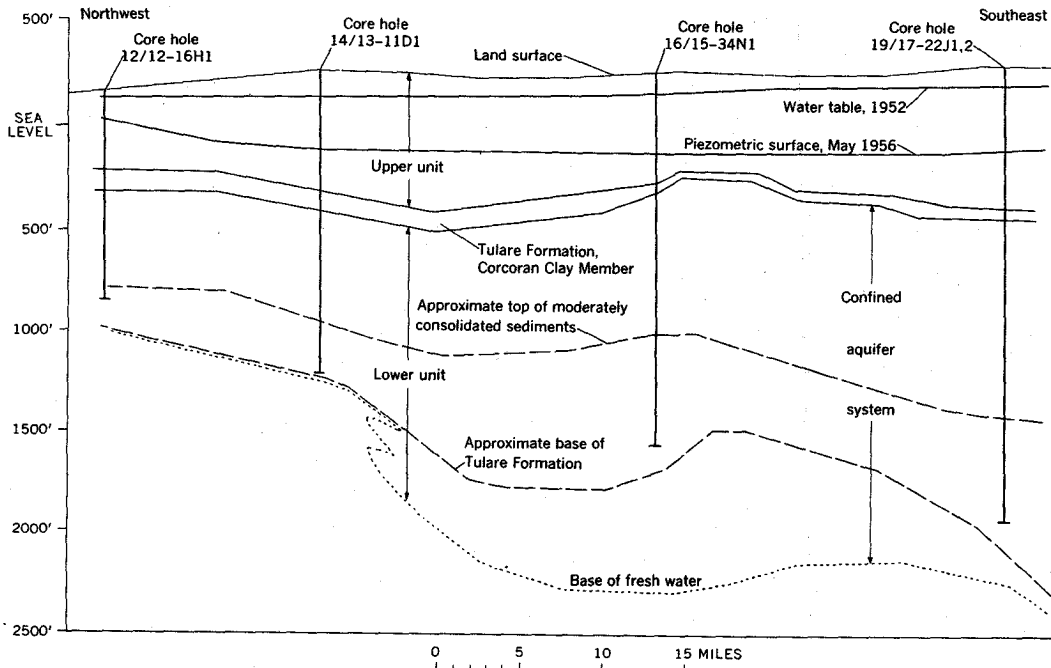


Figure 4.1 Simplified geologic section through core holes in the Los Banos-Kettleman City area, San Joaquin Valley, California.

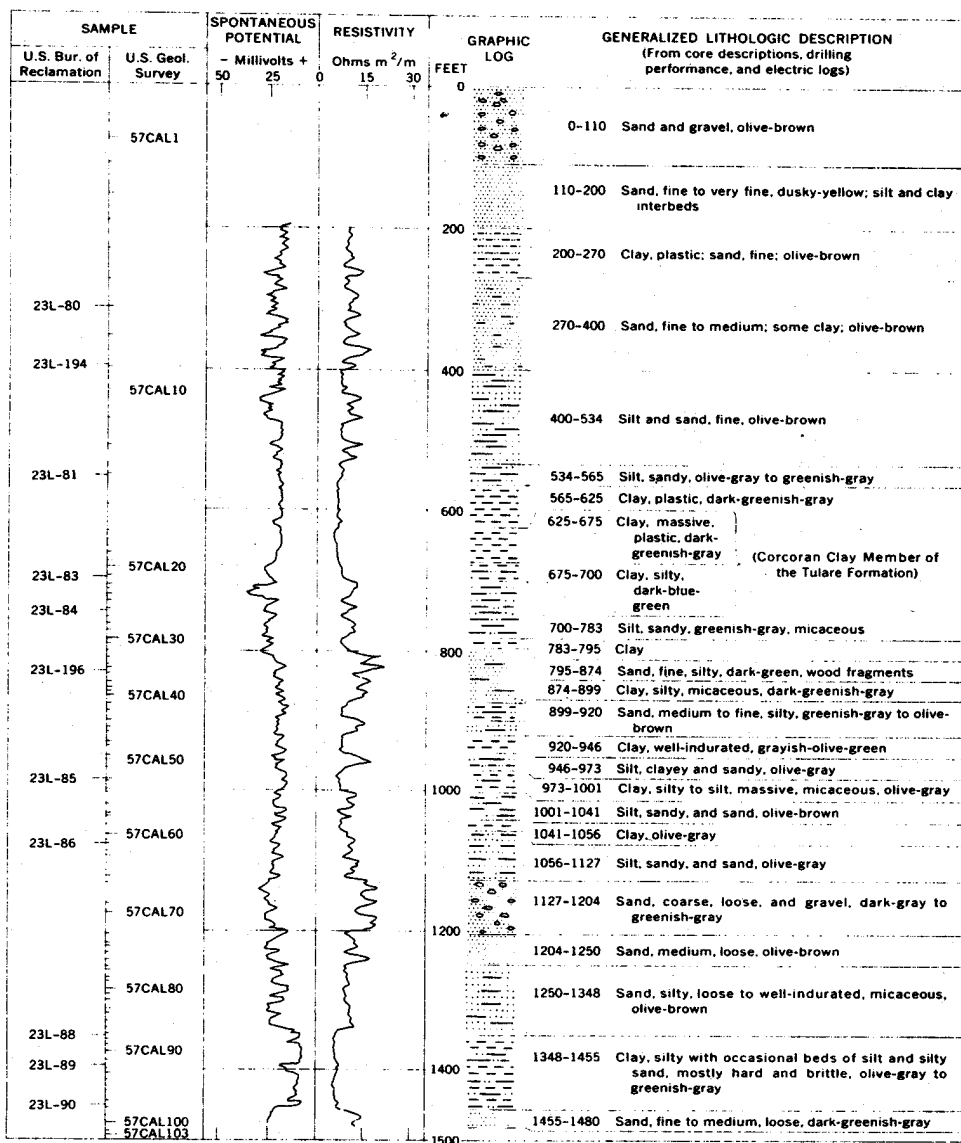
1. Physical and engineering properties sample.--One litre-sized sample (about 15 cm long), taken from the most representative materials of the cored interval, was sealed in wax in a cardboard container to preserve the natural moisture content insofar as practicable and to prevent disturbance of the core.
2. Petrographic samples.--One or more samples, taken from the same materials and contiguous to the physical characteristic samples, were collected and sealed in wax in a 0.5 litre cardboard container and retained for petrographic examination. For paleontologic examination, samples also were taken of fossiliferous beds encountered in several of the core holes; they were not sealed in wax.
3. General purpose samples.--Two or more 0.25 litre samples were collected for general reference, one representing the fine-textured materials and one representing the coarse-textured layers; they were retained in cardboard cartons but not sealed in wax.

In addition, undisturbed samples of representative fine-grained deposits were collected for consolidation tests. Litre-sized samples were carefully selected and then sealed in wax in metal containers to keep them in an undisturbed condition.

#### 4.3 COMPOSITE LOGS OF CORE HOLES

An electric log was obtained for each core hole after coring was completed. Graphic logs and generalized lithologic descriptions were prepared from the geologists' logs made at the drill site, supplemented by interpretation of the electric log in zones not cored or of poor recovery. These three elements were combined to give a composite log for each core hole. The depths of the samples tested also are plotted on the composite logs. Figure 4. 2 is an example of a composite log for one of the core holes.

The interpretation of electric logs is based on the principle that, in fresh-water-bearing deposits such as those penetrated in this area, high resistivity values are indicative of sand and low resistivity values are indicative of clay and silty clay. Intermediate values are indicative of clayey silt, silt, silty sand, and other sediments classified texturally between sand and clay. Resistivity is indicated by the right-hand curve of the electric log; it increases toward the right. Thus, the Corcoran Clay Member of the Tulare Formation is indicated



CORE HOLE 14/13-11DI, LOS BANOS-KETTLEMAN CITY AREA

Figure 4.2 Example of a composite log of a core hole.

by a curve segment of uniformly low resistivity (Figure 4.2). The electric logs of the core holes can be compared with the physical and hydrologic properties of the samples plotted according to depth, as in Figures 4.3 and 4.4.

#### 4.4 METHODS OF LABORATORY ANALYSIS

Utilizing a hydraulic-press assembly in the laboratory, cores 5 cm in diameter by 5 cm long were obtained by forcing thin-wall brass cylinders into the larger core--one in a direction at right angles to the bedding (vertical) and the other parallel to the bedding (horizontal). These small cores were used for permeability tests and for determining unit weight and porosity.

The rest of the large core was prepared and used for determination of specific gravity, particle-size distribution, and Atterberg limits and indices. Sample preparation for these analyses began with the air-drying of chunks of the large core. These chunks of material were

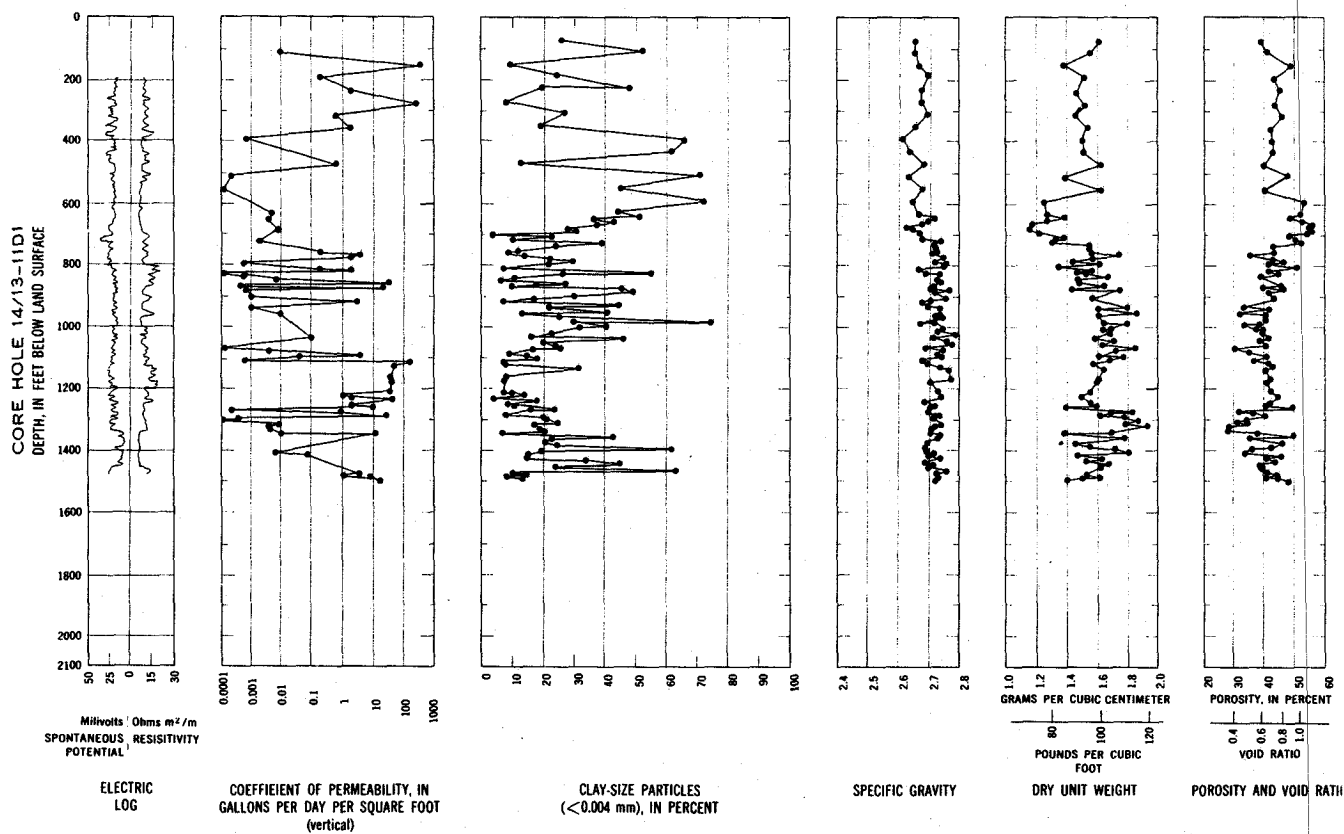


Figure 4.3 A graph of physical properties from core hole 14/13-11D1 in the San Joaquin Valley, California.

then gently but thoroughly separated into individual particles in a mortar with a rubber-covered pestle. Care was taken to prevent crushing of the individual particles.

Core samples were analyzed by use of the standard methods described briefly in the following paragraphs. Additional information on the theory and methods of analysis is available in Meinzer (1923, 1949), Wenzel (1942), Taylor (1948), U.S. Bureau of Reclamation (1974, p. 407-508) and the American Society for Testing Materials (1980). Results of the laboratory analyses were reported in tables. The first page of each of the tables is shown as tables 4.1 through 4.5 at the end of this chapter as an example of the format and type of the data reported. The tables were published in inch-pound units, thus readers interested in metric units may refer to the metric conversion table, Appendix E.

#### 4.4.1 Particle-size distribution

Particle-size analysis, also termed a "mechanical analysis," is the determination of the distribution of particle sizes in a sample. Particle sizes smaller than 0.0625 mm were determined by the hydrometer method of sedimentation analysis, and sizes larger than 0.0625 mm were determined by wet-sieve analysis.

The hydrometer method of sedimentation analysis consisted of (1) dispersing a representative part of the prepared sample with a deflocculating agent, sodium hexametaphosphate, in one litre of water and (2) measuring the density of the suspension at increasing intervals of time with a soil hydrometer. At given times, the size of the largest particles remaining in suspension at the level of the hydrometer was computed by use of Stokes' law, and the weight of particles finer than that size was computed from the density of the suspension at the same level.

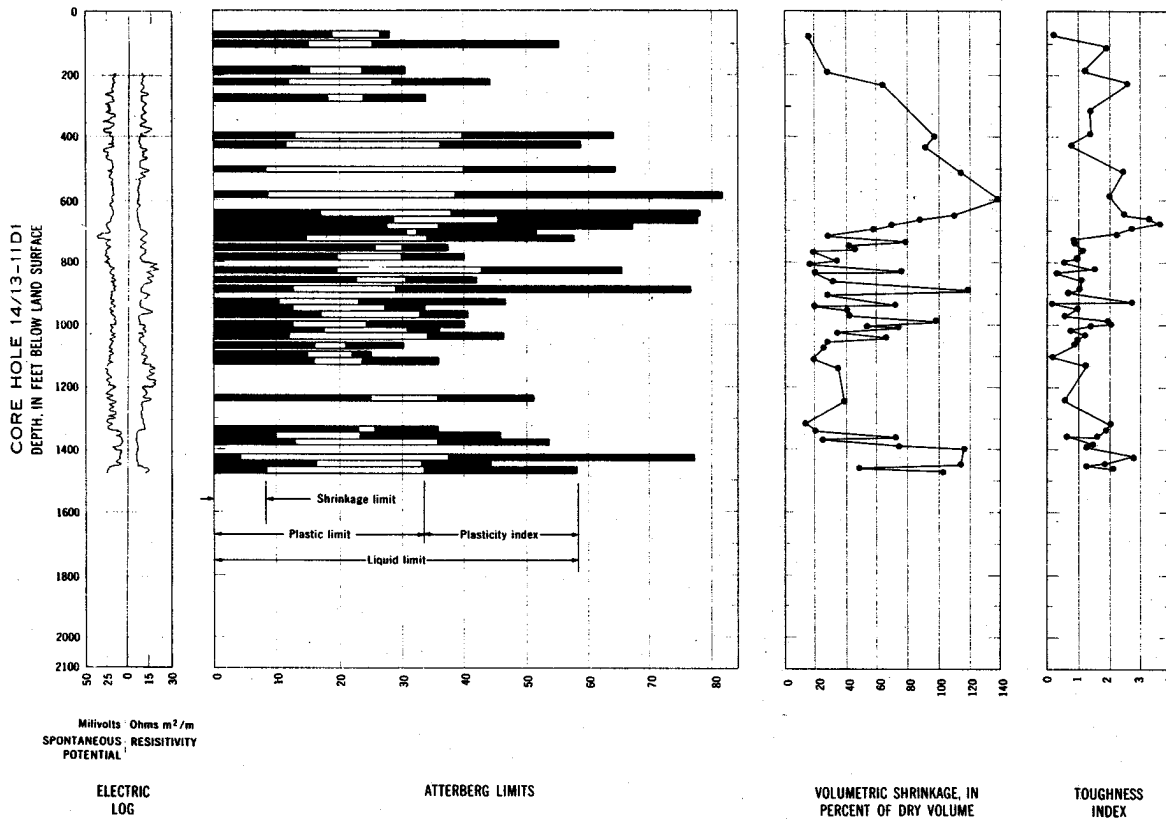


Figure 4.4 Continuation of a graph of properties from core hole 14/13-11D1 in the San Joaquin Valley, California.

After the hydrometer analysis, the sample suspension was poured into a sieve which had openings of 0.0625 mm. The sample then was gently agitated and washed over the sieve. The material retained was carefully dried and placed in a set of standard 20-cm sieves which were shaken for a period of 15 minutes on a Ro-tap mechanical shaker. The fraction of the sample remaining on each sieve was weighed on a balance.

From the hydrometer analysis and the sieve analysis, the percentage of the particles smaller than a given size was calculated and plotted as a cumulative distribution curve. The particle sizes, in millimeters, were plotted as abscissas on a logarithmic scale and the cumulative percentages of particles smaller than the size shown, by weight, as ordinates on an arithmetic scale. The percentage in each of several size ranges was then determined from this curve.

The size ranges were identified according to the following particle sizes:

	Diameter (mm)
Gravel -----	>2.0
Very coarse sand -----	1.0 - 2.0
Coarse sand -----	.5 - 1.0
Medium sand -----	.25 - .5
Fine sand -----	.125 - .25
Very fine sand -----	.0625 - .125
Silt-size -----	.004 - .0625
Clay-size -----	<0.004

This size classification system is used by the Water Resources Division, U.S. Geological Survey, and is essentially the same as classifications proposed by Wentworth (1922) and the National Research Council (Lane, 1947), except that those authors proposed further subdivisions of gravel, silt, and clay. Subsequent references to sand, silt, and clay in this report will relate to sand-, silt-, and clay-size particles as specified in the foregoing table.

#### 4.4.2 Permeability

Permeability is the capacity of rock or soil to transmit fluid under the combined action of gravity and pressure. It can be determined in the laboratory by observing the rate of movement of fluid through a sample of known length and cross-sectional area, under a known difference head.

The basic law for flow of fluids through porous materials was established by Darcy who demonstrated experimentally that the rate of flow of water was proportional to the hydraulic gradient. Darcy's law may be expressed as

$$Q = KiA, \quad (4.1)$$

where  $Q$  is the quantity of water discharged in a unit of time,  $A$  is the total cross-sectional area through which the water flows,  $i$  is the hydraulic gradient (the difference in head,  $h$ , divided by the length of flow,  $L$ ), and  $K$  is the hydraulic conductivity (occasionally known as the coefficient of permeability) of the material for water, or

$$K = \frac{Q}{iA} = \frac{QL}{hA} \quad (4.2)$$

Because the water is assumed to be relatively pure, density is ignored.

Hydraulic conductivity is determined in the laboratory in constant-head or variable-head permeameters or is computed from consolidation-test results. The permeameters used for the tests discussed in this chapter are described in detail by Johnson, Moston, Morris (1968).

Entrapped air in a sample may cause plugging of pore space and thus reduce the apparent hydraulic conductivity. Therefore, a specially designed vacuum system provided the de-aired tapwater used as the percolation fluid.

The chemical character of the water used for the permeability tests of fine-grained silty or clayey materials should be compatible with the chemical character of the native pore water. If the test water is not compatible, the clay-water system and the permeability values obtained will be affected. The chemical character of the native pore water in the fine-grained sediment was not known at the time of the test and Denver tapwater therefore was used in the permeability tests.

The 5-cm-diameter "undisturbed" cores cut from the larger original core were retained in their cylinders. These cylinders were installed directly in the permeameter to serve as the percolation cylinder of the apparatus. The reported hydraulic conductivity was the maximum value obtained after several test runs and represents saturation permeability.

#### 4.4.3 Unit weight

For reference in developing some of the equations used in following sections of this chapter, it is useful to study the relations found in a unit soil mass, as seen in Figure 4 5. The concepts and symbols shown in that figure will be used in development of equations related to the properties of compacting sediments. Other useful definitions and symbols can be found in the publication of the American Society for Testing and Materials (1980).

The dry unit weight is the weight of solids per unit of total volume of oven-dry rock or soil mass. It normally is reported in grams per cubic centimeter or kilograms per cubic metre. Void space as well as solid particles are included in the volume represented by the dry unit weight. The dry unit weight divided by the unit weight of distilled water at a stated temperature (usually 4° C) is known occasionally as the apparent specific gravity, which is dimensionless.

The volume of the small cores, cut previously from the large cores, was obtained by measurement of the cylinder dimensions. This volume and the oven-dry weight of the contained sample were then used to calculate the dry unit weight as follows:

$$\gamma_d = \frac{W_s}{V}, \quad (4.3)$$

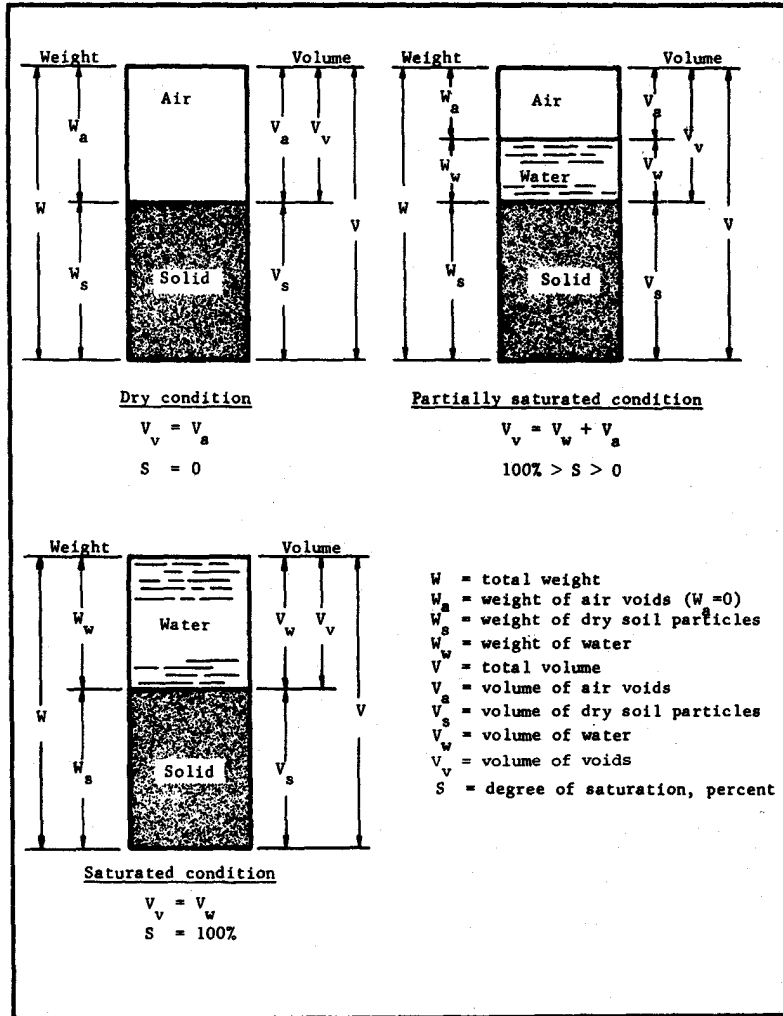


Figure 4.5 Principal phases of a unit soil mass.

where

- $\gamma_d$  = dry unit weight, in grams per cubic centimetre,
- $W_s$  = weight of oven-dry sample, in grams,
- $V$  = total mass volume of sample, in cubic centimetres.

#### 4.4.4 Specific gravity of solids

Specific gravity of solids,  $G$ , is the ratio of (1) the weight in air of a given volume of solids at a stated temperature (unit weight of solid particles or particle density) to (2) the weight in air of an equal volume of distilled water at stated temperature (usually 4° C), or

$$\gamma_s = \frac{W_s}{V_s} \quad \text{and} \quad \gamma_w = \frac{W_w}{V_w} ,$$

so

$$G = \frac{\gamma_s}{\gamma_w} \tag{4.4}$$

where

$\gamma_s$  = unit weight of solids, in grams per cubic centimetre,  
 $V_s$  = volume of solids, in cubic centimetres,  
 $\gamma_w$  = unit weight of water, in grams per cubic centimetre,  
 $W_w$  = weight of water, in grams,  
 $V_w$  = volume of water, in cubic centimetres, and  
 $G$  = specific gravity, a ratio.

The volumetric-flask method was used for determining the specific gravity of solids. A weighed oven-dry part of the sample was dispersed in water in a calibrated volumetric flask. The volume of the particles was equivalent to the volume of displaced water. The unit weight of the solid particles was obtained by dividing the dry weight of the sample by the volume of the solid particles. Because the density of water at 4° C is unity in the metric system, the specific gravity is numerically equivalent to this unit weight.

#### 4.4.5 Porosity and void ratio

Porosity,  $n$ , is defined as the ratio of (1) the volume of the void spaces to (2) the total volume of the rock or soil mass. It normally is expressed as a percentage. Therefore,

$$n = \frac{V_v(100)}{V} = \frac{V - V_s(100)}{V}, \quad (4.5)$$

then as

$$\gamma_d = \frac{W_s}{V}$$

and

$$\gamma_s = \frac{W_s}{V_s},$$

$$n = \frac{W_s/\gamma_d - W_s/\gamma_s}{W_s/\gamma_d}(100),$$

or

$$n = \frac{\gamma_s - \gamma_d}{\gamma_s}(100) \quad (4.6)$$

where

$n$  = porosity, in per cent,  
 $V_v$  = volume of voids, in cubic centimetres,  
 $V$  = total mass volume, in cubic centimetres,  
 $W_s$  = weight of oven-dry particles, in grams,  
 $\gamma_s$  = unit weight of particles, in grams per cubic centimetre (equal numerically to specific gravity of solids in metric system),  
 $\gamma_d$  = dry unit weight of sample, in grams per cubic centimetre, and  
 $V_s$  = volume of solid particles, in cubic centimetres.

After the dry unit weight and the specific gravity of solids had been determined for the sample, the porosity was calculated from the above equation. The relation among these three properties is illustrated in Figure 4.6.

The void ratio is defined as the ratio of (1) the volume of voids to (2) the volume of solid particles in a soil mass, or

$$e = \frac{V_v}{V_s} \quad (4.7)$$

Its relation to porosity is expressed by

$$e = \frac{n}{1-n}, \quad (4.8)$$

where  $e$  = void ratio, and  $n$  = porosity, in per cent.

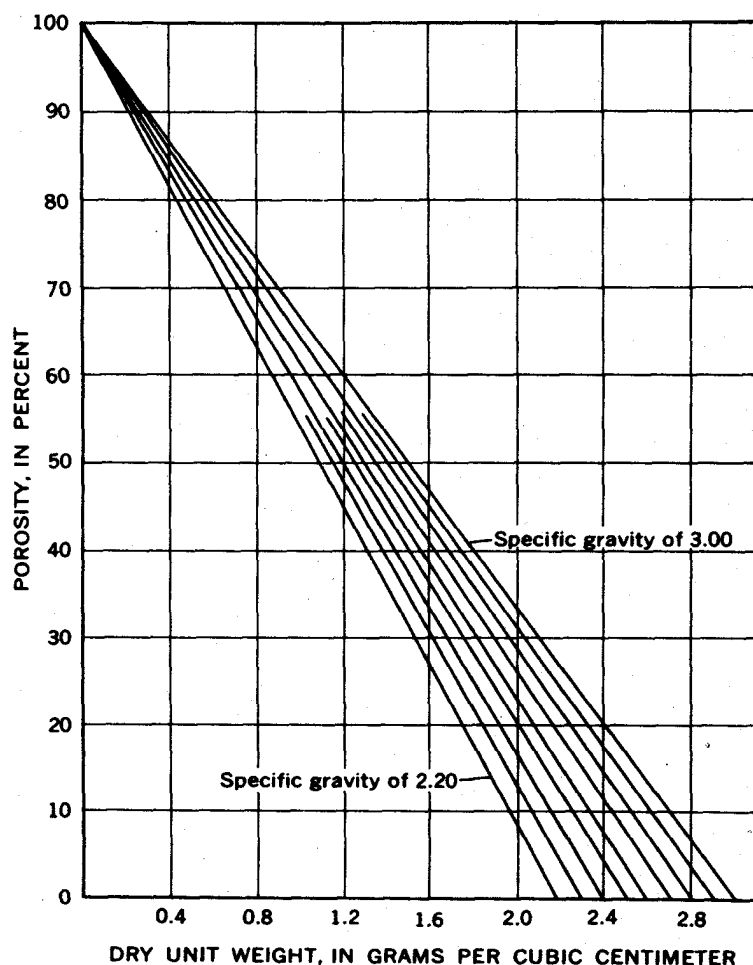


Figure 4.6 Relation of porosity to dry unit weight for various specific gravities of solids.

The relation between void ratio and porosity is illustrated in Figure 4.7.

#### 4.4.6 Moisture content

The moisture content of rock or soil material is the ratio of the weight of water contained in a sample to the oven-dry weight of solid particles, expressed as a percentage, or

$$w = \frac{W_w}{W_s}(100), \tag{4.9}$$

where

- w = moisture content, in per cent of dry weight,
- $W_w$  = weight of water, in grams, and
- $W_s$  = weight of oven-dry sample (dry solids), in grams.

Usually, samples in moisture-proof containers, are weighed to obtain their wet weight. They are oven-dried to constant weight at 110°C and reweighed. The loss of weight (the amount of contained water) divided by the dry weight of the sample equals the moisture content.

#### 4.4.7 Atterberg limits

Atterberg (1911), a Swedish soil scientist, suggested a series of arbitrary limits for indicating the effects of variations of moisture content on the plasticity of soil materials.

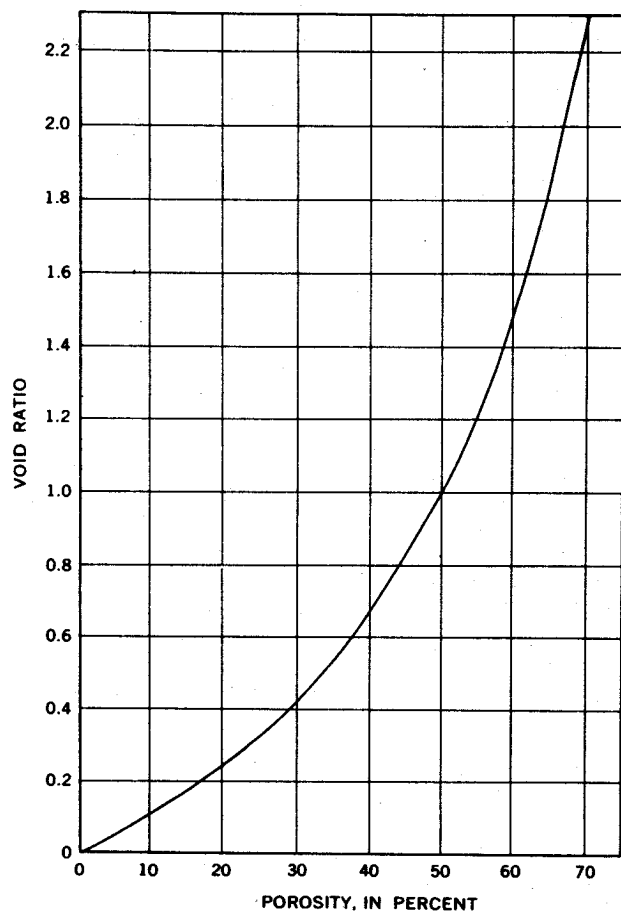


Figure 4.7 Relation of void ratio to porosity.

The most commonly used Atterberg limits, sometimes referred to as limits of consistency, are the liquid and plastic limits. Among a number of indices, the plasticity index is most commonly determined.

The moisture contents at which fine-textured sediments pass from one state of consistency to another are governed by the texture and composition of the sediments. Atterberg (1911), Terzaghi (1926), and Goldschmidt (1926) found that plasticity is a function of the amount of fine platelike particles in a sediment mass. Thus, the Atterberg consistency limits and indices are influenced by the clay content of the sediments tested.

Although the Atterberg limits are somewhat empirical, most soil investigators believe that they are valuable in characterizing the plastic properties of fine-textured sediment, (Casagrande, 1932).

Only the smaller size particles of a given sample, those passing a U.S. Standard No. 40 sieve (finer than 0.42 mm in diameter) are used for Atterberg tests. Although limits and indices are calculated as moisture content, in per cent of dry weight, ( $W_w/W_s$ ), all values are usually reported as numbers only.

#### 4.4.7.1 Liquid limit

The liquid limit,  $w_L$ , is the moisture content, expressed as a percentage of the oven-dry weight, at which any particular soil material passes from the plastic to the liquid state. It is that moisture content at which a groove of standard dimensions cut in a pat of soil will close for a distance of 1/2 in. (1.3 cm) under the impact of 25 shocks in a standard liquid-limit apparatus. The moist sample was placed in the round-bottomed brass cup of the mechanical liquid-limit device and was divided into two halves by a V-shaped grooving tool. A cam on the device raised the cup and let it drop against the base of the machine until the two edges of the groove flowed

together for the specified half an inch. The number of taps, or shocks, were recorded, and the moisture content of a part of the sample was determined. This process was repeated three times at different moisture contents. These data are plotted as a "flow curve" on a semilogarithmic graph, the number of shocks plotted as abscissa on the logarithmic scale and the moisture content as ordinates on the arithmetic scale. The moisture content corresponding to the intersection of the flow curve with the 25-shock line was taken as the liquid limit of that soil material.

#### 4.4.7.2 Plastic limit

The plastic limit,  $w_p$ , is the minimum moisture content, expressed as a percentage of the oven-dry weight, at which soil material can be rolled into 1/8-in. (0.3-cm) diameter threads without the threads breaking into pieces. This moisture content represents the transition point between the plastic and semisolid states of consistency. The moist sample was rolled between the hand and a glass plate until a thread 0.3 cm in diameter was formed. The sample was then kneaded together and again rolled out. This process was continued at slowly decreasing water contents until crumbling prevented the formation of the thread. The pieces of the crumbled sample were then collected together and the moisture content was determined. This moisture content was considered to be the plastic limit.

#### 4.4.8 Consolidation

When a saturated soil sample is subjected to a load, that load initially is carried by the water in the voids of the sample because the water is incompressible in comparison with the sample's structure. If water can escape from the sample voids as a load is continually applied to the sample, an adjustment takes place wherein the load is gradually shifted to the soil structure. This process of load transference is generally slow for clay and is accompanied by a change in volume of the soil mass. Consolidation is defined as that gradual process which involves, simultaneously, a slow escape of water, a gradual compression, and a gradual pressure adjustment. This use of the term should not be confused with the geologists' definition which refers to the processes by which a material becomes firm or coherent (Am. Geol. Inst., 1957, p. 62). The theory of consolidation is discussed in detail by Terzaghi (1943, p. 265-297).

To determine the rate and magnitude of consolidation of sediments, a small-scale laboratory test known as a one-dimensional consolidation test is used. The test and apparatus, described in detail by the U.S. Bureau of Reclamation (1974), are discussed briefly in the following paragraphs for the benefit of the reader. The application of one-dimensional consolidation test data to a foundation-settlement analysis has been described by Gibbs (1953). The apparatus (consolidometer) used by the Bureau of Reclamation (1974) is shown in Figure 4.8. In addition to the unit shown, a means of loading is required--usually a platform scale with a weighing beam attached to the connecting rods of the consolidometer.

Normally, the sample is trimmed to the size of the specimen rings, which are 4-1/4 in. (10.8 cm) in inside diameter and 1-1/4 in. (3.2 cm) high. Samples must be in as near an undisturbed condition as possible. Because of the small size of the cores collected for the subsidence studies, however, consolidation specimens of standard size could not be used, and the core diameter had to be trimmed to fit 2 in. (5-cm) rings.

Loads are applied to the specimen in increments, but the minimum number of increments is usually four-- 12, 25, 50, and 100 per cent of the maximum desired load. Increments are usually selected so that each succeeding load is double that of the previous load. Each load is applied to the consolidometer while dial readings of consolidation are taken and recorded for 4, 10, 20 seconds, and other time intervals up to 24 hours. Additional readings are taken at 24-hour intervals until the consolidation is virtually complete for that load.

The percentage of consolidation of the specimen is computed, and a curve of consolidation versus time is obtained for each load increment. The final stress-strain relations are presented as a curve showing the void ratio versus log of pressure (load), the final condition for each increment of load being a point on the curve (Figure 4.9).

Two important soil properties furnished by a consolidation test are the coefficient of consolidation and the compression index. The coefficient of consolidation,  $C_v$ , represents the rate of consolidation for a given load increment. It is determined by use of the 50-percent point on the time consolidation curve in the equation

$$C_v = \frac{T_{50}^2}{t_{50}}, \quad (4.10)$$

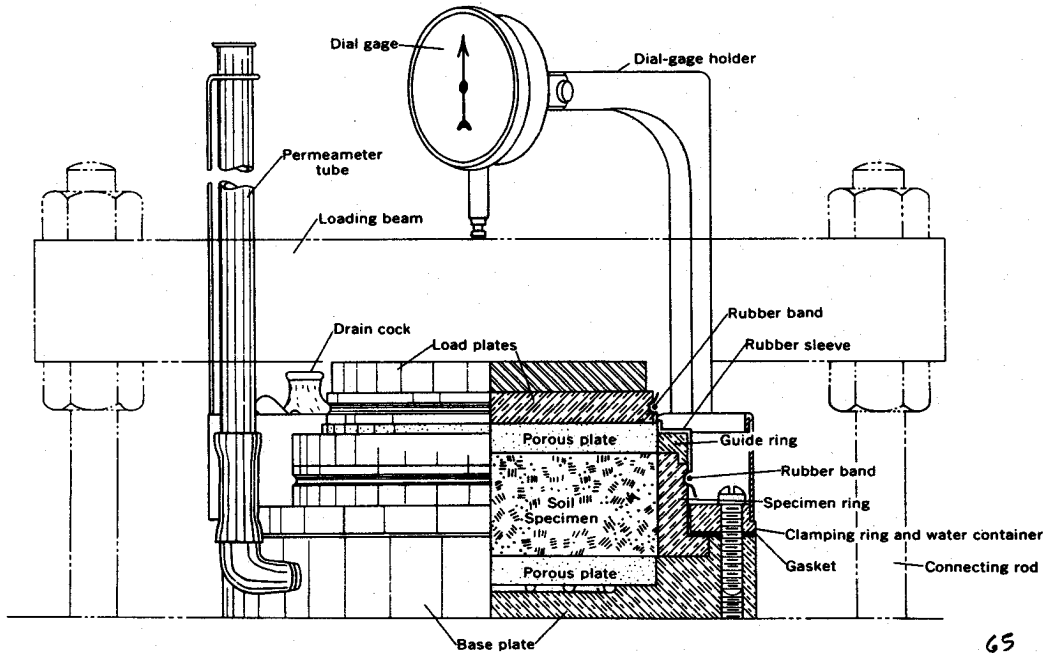


Figure 4.8 One-dimensional consolidometer specimen container (from U.S. Bureau of Reclamation, 1960, p. 495).

where

$T_{50}$  = time factor at 50-per-cent consolidation = 0.20,

$H_{50}$  = one half the specimen thickness at 50-per-cent consolidation, and

$t_{50}$  = time required for specimen to reach 50-per-cent consolidation. The coefficient of consolidation is usually reported in square centimetres per second or in square inches per second.

The compression index,  $C_c$ , represents the compressibility of the soil samples. It is the slope of the straight-line portion of the void ratio-log of pressure (load) curve. The compression index can be determined from the equation

$$C_c = \frac{e_o - e}{\log \frac{P_o + \Delta P}{P_o}} \quad (\text{see Figure 4.9 for symbols}). \quad (4.11)$$

When the consolidation is complete under maximum loading, the consolidometer can be used as a variable-head permeameter, and the hydraulic conductivity can be determined directly. The mechanical procedure is similar to that described previously (section 4.4.2). The consolidation data also can be used for computing the hydraulic conductivity. The equation utilizing time-consolidation characteristics is

$$K = \frac{C_v(\gamma_w)(e_o - e)}{\Delta_p(1 + e_o)} \quad (4.12)$$

where

$C_v$  = coefficient of consolidation,

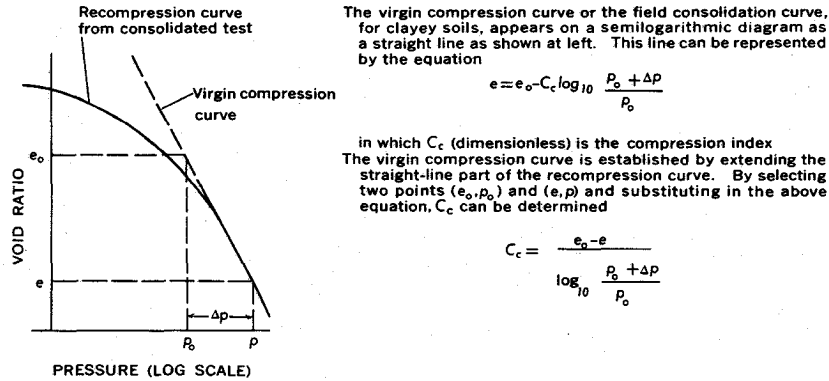
$\gamma_w$  = unit weight of water,

$e_o$  = void ratio at start of load increment,

$e$  = final void ratio, and

$\Delta_p$  = increment of load.

Although the example in Table 4.4 shows feet per year for the permeability (standard inch-pound system units), cm per sec is the commonly reported unit for  $K$ .



A. METHOD OF DETERMINING THE COMPRESSION INDEX ( $C_c$ )

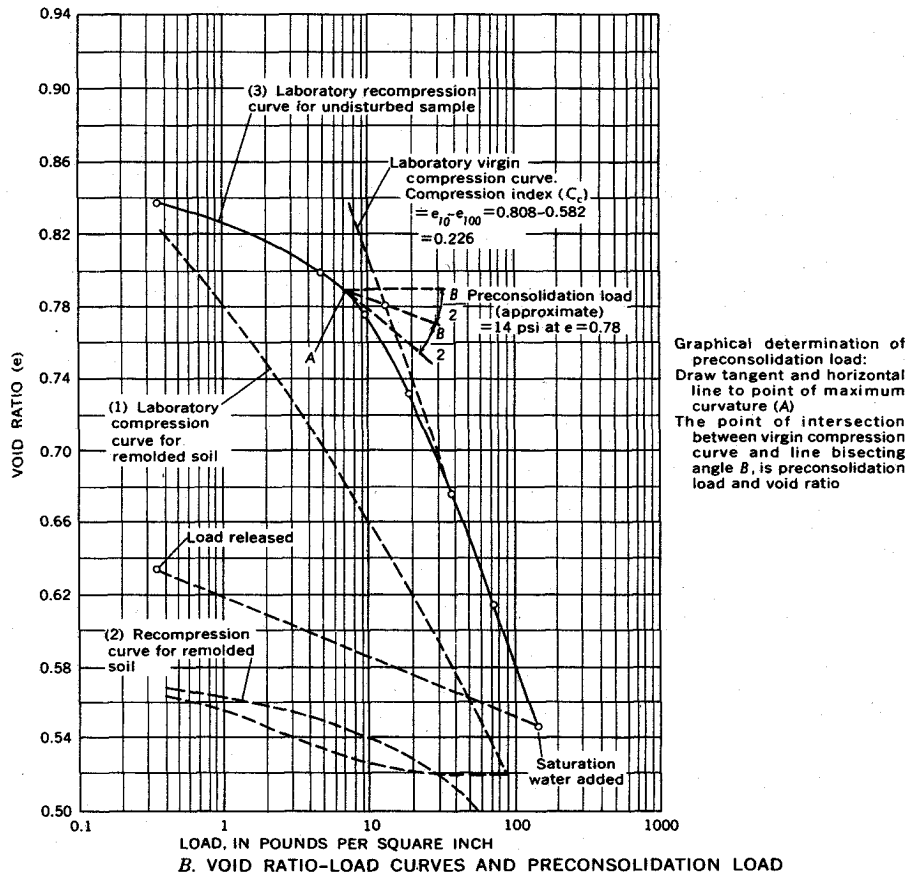


Figure 4.9 Void ratio-load curve, compression index, and preconsolidation load (modified from U.S. Bureau of Reclamation, 1960, p. 58).

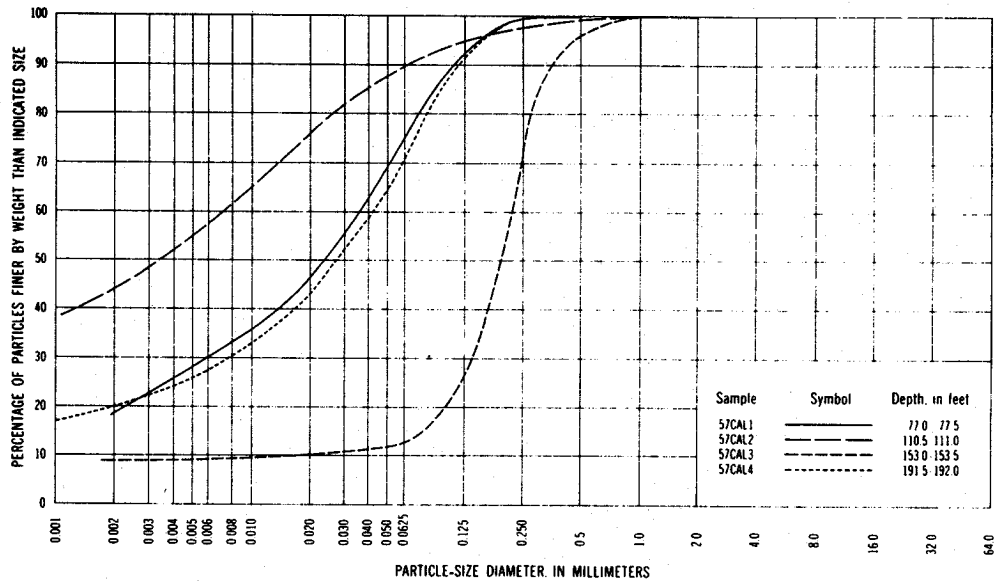
4.5 RESULTS OF LABORATORY ANALYSES

4.5.1 Particle-size distribution

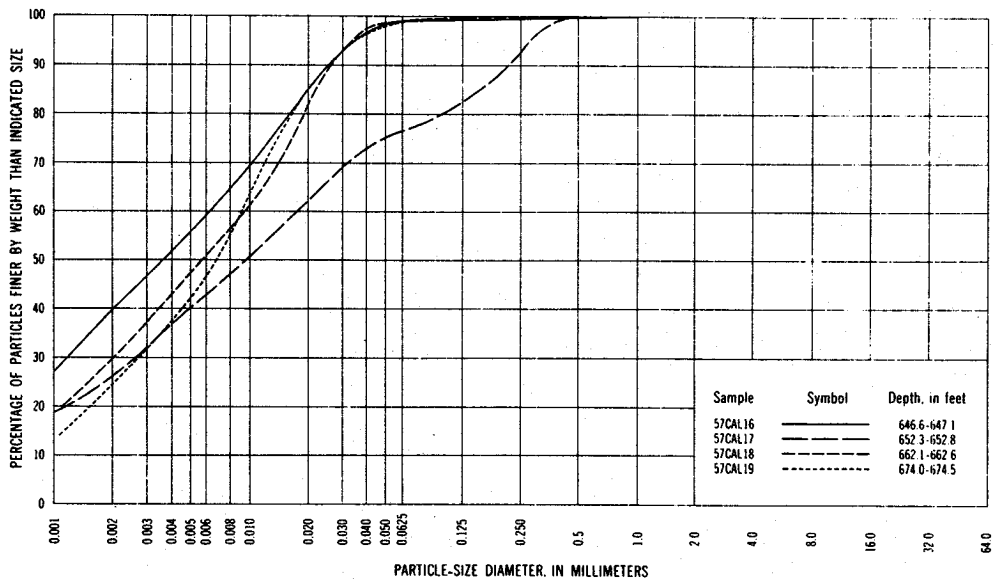
An example of particle-size distribution data from central California is presented in Table 4.1. The percentage of gravel-, sand, silt-, and clay-size particles were shown in such tables for each of the 549 samples from seven core holes analyzed in the laboratory. Particle-size distribution curves for all of the samples were plotted on figures similar to Figure 4.10. An example of the size-distribution (gradation) for samples tested for consolidation is given in Table 4.3.

Table 4.1 Physical and hydrologic properties of samples from core holes.

Hydrologic laboratory sample	Sample depth (feet)	Particle analysis, percentage of—			Median diameter, $D_{50}$ (mm)	Geometrical quartile deviation (sorting coefficient), $S_o$	Log quartile deviation (log sorting coefficient), $\log_{10} S_o$	Sediment class (Shepard system)	Specific gravity of solids	Dry unit weight		Total porosity (percent)	Void ratio	Coefficient of permeability (cp per sq ft at 60°F)	
		Gravel	Sand	Silt						Clay <0.004 mm	Clay <0.002 mm			Vertical	Horizontal
ETCAL1	77.0-110.5		24.8	49.5	0.024	4.04	0.606	Sand-silt-clay	2.66	1.60	39.9	0.69	0.01	0.03	
2	110.5-153.0		10.7	52.0	0.034	4.04	0.606	Sand-silt-clay	2.66	1.56	41.4	0.71	0.01	0.03	
3	153.0-191.5		87.1	37.3	0.19	3.92	1.64	Sand	2.67	1.37	85.5	0.71	390	2	
4	191.5-232.5		26.0	46.8	0.028	3.82	0.593	Sand-silt-clay	2.67	1.52	48.7	0.78	2	2	
5a	232.5-283.0		21.6	30.4	0.045	3.16	0.500	do.	2.68	1.47	45.1	0.82	2	4	
5b	283.0-314.5		89.0	18.9	0.092	3.16	0.500	Clayey sand	2.68	1.64	37.9	0.81	270	6	
6	314.5-348.0	1.3	89.0	1.9	0.25	4.12	0.201	Sand	2.68	1.52	43.3	0.85	2	2	
7	348.0-383.0		22.3	26.7	0.019	4.12	0.613	Sand-silt-clay	2.70	1.46	41.1	0.73	2	2	
8	383.0-417.0		41.0	38.3	0.060	3.37	0.528	Sand-silt-clay	2.66	1.54	42.4	0.74	2	2	
9	417.0-452.0		7.0	31.2	0.030	2.00	0.301	Silty sand	2.62	1.51	44.2	0.71	7	0.007	
10	452.0-487.0		47.3	40.0	0.089	2.00	0.301	Silty sand	2.64	1.63	36.7	0.65	7	0.007	
11	487.0-510.8		47.3	40.0	0.089	2.00	0.301	Silty sand	2.64	1.63	36.7	0.65	7	0.007	
12	510.8-550.0	6	8.9	19.5	0.062	5.68	0.754	Sand-silt-clay	2.65	1.39	39.2	1.12	0.001	0.001	
13	550.0-594.5		22.0	33.0	0.032	5.68	0.754	Sand-silt-clay	2.65	1.25	52.8	1.09	0.005	0.005	
14	594.5-631.5		8.8	19.7	0.057	5.68	0.754	Sand-silt-clay	2.67	1.28	52.1	1.09	0.005	0.005	
15	631.5-647.1		19.2	36.3	0.036	5.68	0.754	do.	2.72	1.30	46.9	1.11	0.004	0.004	
16	647.1-662.8		1.0	47.5	0.006	5.68	0.754	do.	2.68	1.18	52.6	1.11	0.004	0.004	
17	662.8-692.8		23.3	40.1	0.096	5.68	0.754	Sand-silt-clay	2.68	1.28	46.9	1.09	0.004	0.004	
18	692.8-717.5		8.8	56.2	0.038	5.68	0.754	Sand-silt-clay	2.68	1.18	52.6	1.11	0.004	0.004	
19	717.5-743.5		1.0	61.5	0.008	5.68	0.754	do.	2.65	1.17	55.8	1.23	0.008	0.008	
20	743.5-769.5		1.0	61.5	0.008	5.68	0.754	do.	2.65	1.17	55.8	1.23	0.008	0.008	
21	769.5-791.5		26.8	48.2	0.042	5.68	0.754	Sand-silt-clay	2.67	1.23	54.1	1.18	0.008	0.008	
22	791.5-802.5		80.2	18.1	0.282	2.00	0.301	Silt	2.68	1.33	48.4	1.04	0.002	0.002	
23	802.5-828.5		80.2	18.1	0.282	2.00	0.301	Silt	2.68	1.33	48.4	1.04	0.002	0.002	
24	828.5-844.5		1.0	72.8	0.010	2.00	0.301	Silt	2.72	1.55	52.2	1.10	0.002	0.002	
25	844.5-875.5		4.0	88.0	0.010	2.00	0.301	Silt	2.72	1.55	52.2	1.10	0.002	0.002	
26	875.5-900.5		1.6	86.4	0.007	2.00	0.301	Silt	2.72	1.55	52.2	1.10	0.002	0.002	
27	900.5-928.5		6.0	70.0	0.013	2.57	0.410	Silty sand	2.73	1.57	42.9	1.09	4	2	
28	928.5-953.5		3.8	77.4	0.062	2.57	0.410	Silty sand	2.73	1.57	42.9	1.09	4	2	
29	953.5-977.5		50.2	38.1	0.34	2.42	0.384	Sand	2.71	1.45	35.4	1.11	4	2	
30	977.5-1000.5		77.4	13.9	0.50	2.22	0.346	Sandy silt	2.75	1.45	30.7	1.09	4	2	
31	1000.5-1028.5		16.2	61.8	0.020	2.94	0.468								



PERCENT OF PARTICLES OF INDICATED SIZE	CLAY 0.004	SILT 0.004 0.0625	SAND					GRAVEL				
			Very fine 0.0625-0.125	Fine 0.125-0.25	Medium 0.25-0.5	Coarse 0.5-1	Very coarse 1-2	Very fine 2-4	Fine 4-8	Medium 8-16	Coarse 16-32	Very coarse 32-64
—	25.7	49.5	16.6	7.0	1.2							
—	52.0	37.3	5.5	2.8	1.6	0.7						
—	9.2	3.7	13.6	42.6	26.7	4.2						
—	24.2	46.8	20.6	8.2	0.2							



PERCENT OF PARTICLES OF INDICATED SIZE	CLAY 0.004	SILT 0.004 0.0625	SAND					GRAVEL				
			Very fine 0.0625-0.125	Fine 0.125-0.25	Medium 0.25-0.5	Coarse 0.5-1	Very coarse 1-2	Very fine 2-4	Fine 4-8	Medium 8-16	Coarse 16-32	Very coarse 32-64
—	51.5	47.5	0.2	0.2	0.2	0.4						
—	36.6	40.1	6.0	9.7	7.6							
—	43.0	56.2	0.2	0.2	0.4							
—	37.5	61.5	0.4	0.2	0.2	0.2						

Figure 4.10 Some graphs of particle-size distribution curves for core hole 14/13-11D1 in the San Joaquin Valley, California.

Because clay content has an important influence on many of the properties of sediments, the clay content for all the samples was plotted to facilitate comparison with the other properties (see example, Figure 4.3). In Table 4.1, the percentage of particles smaller than 2- $\mu\text{m}$  (0.002-mm) clay, as well as smaller than 4- $\mu\text{m}$  (0.004-mm) clay, has been reported. When the 4- $\mu\text{m}$  rather than the 2- $\mu\text{m}$  size was used as the criterion, 78.5 per cent of the samples showed less than 10 per cent greater clay content. In addition, 20.9 per cent of the samples showed 10-20 per cent greater clay content and 0.6 per cent of the samples showed more than 20 per cent greater clay content for the 4- $\mu\text{m}$  than for 2- $\mu\text{m}$  size criterion.

#### 4.5.2 Sediment classification triangles

Most clastic sediments are a mixture of sand-, silt-, and clay-size particles in varying proportions. A suitable nomenclature for sediments is therefore important to describe the approximate relations among these three main constituents. Because sediment classification is often based on the relative percentages of sand-, silt-, and clay-size particles, it is convenient to plot these three constituents on a triangular chart.

A large number of triangular classification systems have been devised over the years. Some were developed primarily for the use of geologists in relating classification to sedimentation characteristics, and others were developed for the use of soils engineers in relating classification to the engineering properties of the sediments. Shepard (1954) developed a sediment classification triangle based on the needs of sedimentologists for studying mode of transport and environment of deposition of sediments. Shepard's classification gives equal importance to sand-, silt-, and clay-size particles (Figure 4.11).

Because the mode of transport and environment of deposition of the sediments were being studied, as well as the engineering properties, Shepard's classification was used in the central California study to determine the sediment class name listed for each sample in Table 4.1. For classification of sediments in the lower Mississippi Valley, the U.S. Army Corps of Engineer (Casagrande, 1948) developed a triangle which emphasizes the importance of clay-size particle content. To assist soils engineers in relating the classification of samples to their engineering properties, a transparent overlay of the Mississippi valley classification triangle could be placed over the plots in Figure 4.11 to determine the classification name under that system.

The textural classification used in Table 4.1, based on the Shepard system, is a laboratory classification derived from particle-size distribution graphs. It departs substantially from the field description made from examination of cores and drill cuttings by geologists especially for the fine-textured materials. In the field examination, material containing more than 30-40 per cent of clay-size particles has sufficient clay content to give it the physical properties of clay, such as plasticity. Therefore, the textural description of cores or samples in the field by geologists is not directly comparable to the laboratory textural classification by the Shepard system. Field examination by the geologists results in a textural description much closer to that of the Mississippi Valley classification than to that of the Shepard classification.

#### 4.5.3 Statistical measures

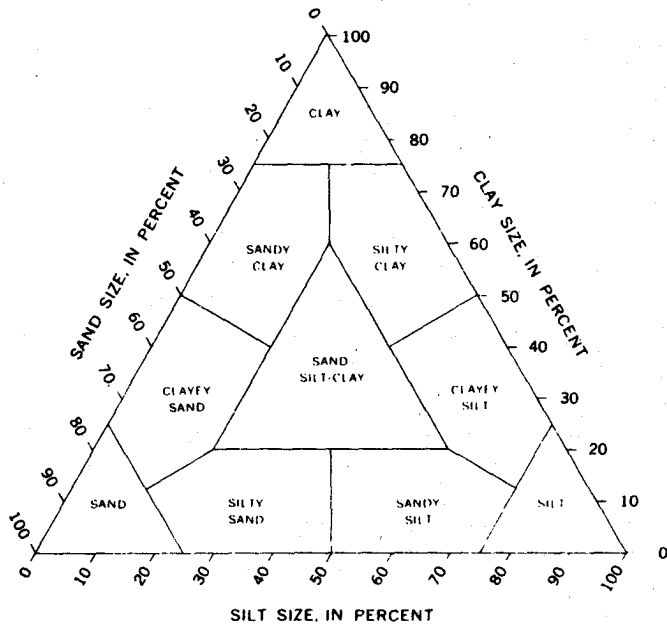
For comparison and statistical analysis, it is convenient to have characteristics of particle-size distribution (mechanical analysis) curves expressed as numbers.

The measure of central tendency is the value (size of particle) about which all other values (sizes) cluster. One such measure is the median diameter,  $D_{50}$ , which is defined as that particle diameter which is larger than 50 per cent of the diameters and smaller than the other 50 per cent. It is determined by reading, from the particle-size distribution curve, the particle diameter at the point where the particle-size distribution curve intersects the 50-percent line.

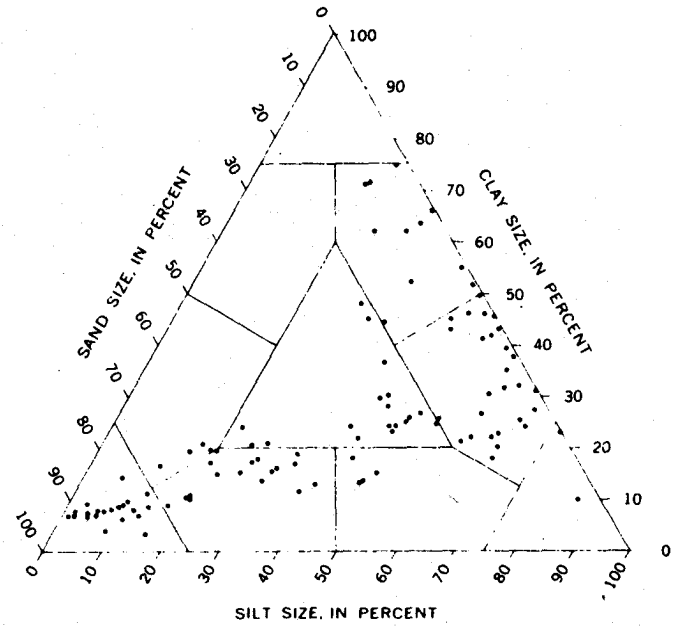
The quartile deviation is a measure of spread of particle sizes. Quartiles are the particle-diameter values read at the intersection of the curve with the 25- ( $Q_1$ ), 50- ( $Q_2$ ), and 75- ( $Q_3$ ) per-cent lines. By convention, the third quartile ( $Q_3$ ) is always taken as the larger value, regardless of the manner of plotting. The geometrical quartile deviation, or the "sorting coefficient,"  $S_o$  of Trask (1932, p. 70-72), is represented by the equation

$$S_o = \sqrt{Q_3/Q_1} \quad (4.13)$$

An  $S_o$  value of less than 2.5 indicates a well-sorted sediment, of 3 a normally sorted sediment, and of 4.5 a poorly sorted sediment.

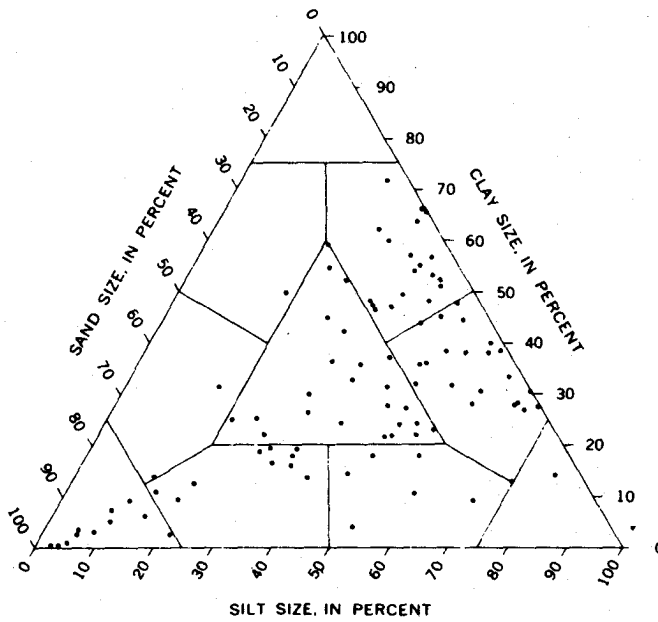


TRIANGULAR PARTICLE-SIZE DIAGRAMS ARE SUBDIVIDED ACCORDING TO THE SYSTEM PROPOSED BY SHEPARD (1954)

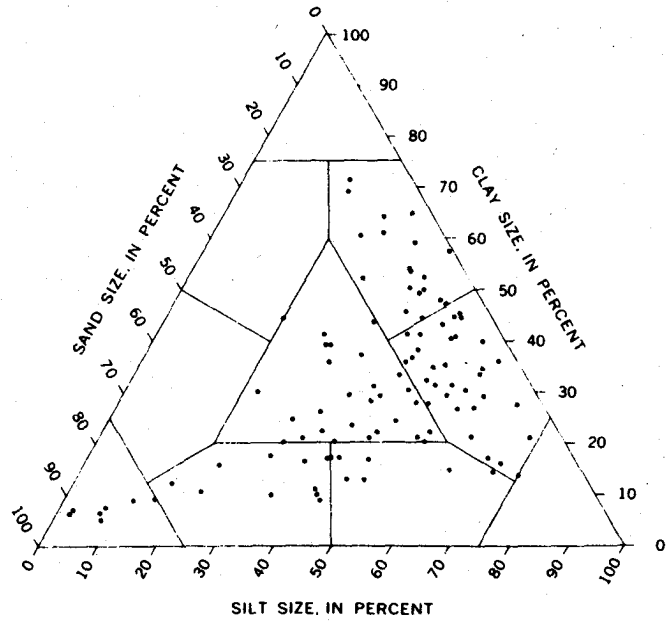


CORE HOLE 14/13-11D1

Sand 2-0.0625  
 Silt 0.0625-0.004  
 Clay . 0.004



CORE HOLE 16/15-34N1



CORE HOLE 19/17-22J1.2

Figure 4.11 Sediment classification triangles for samples from core holes in the Los Banos-Kettleman City area, California.

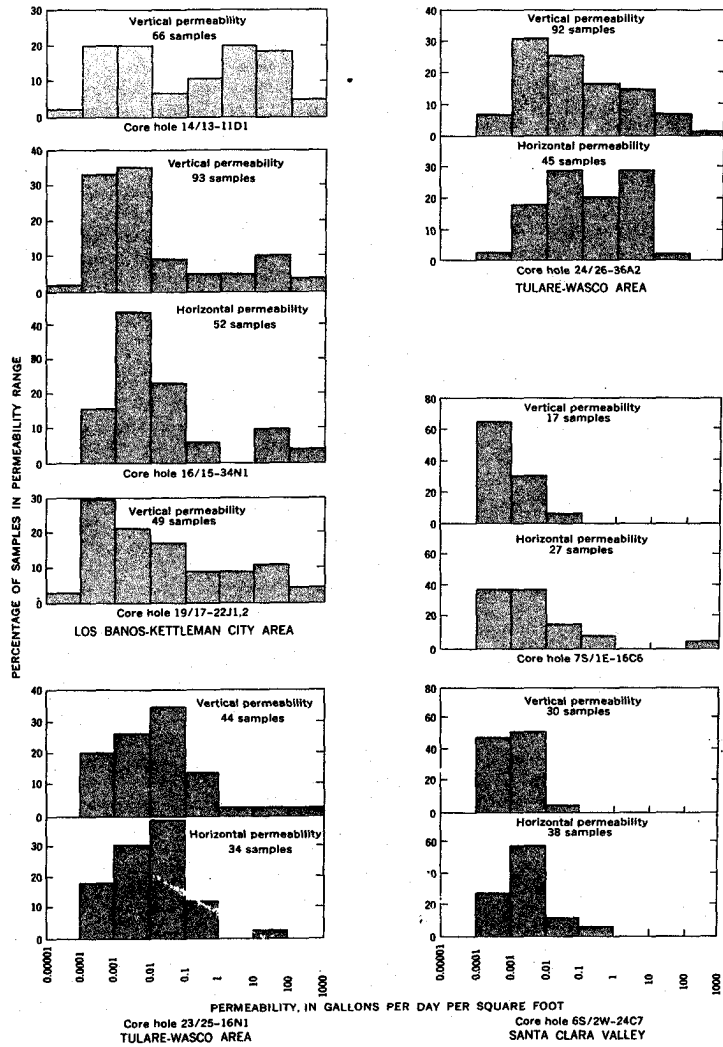


Figure 4.12 Range in permeability of samples from core holes.

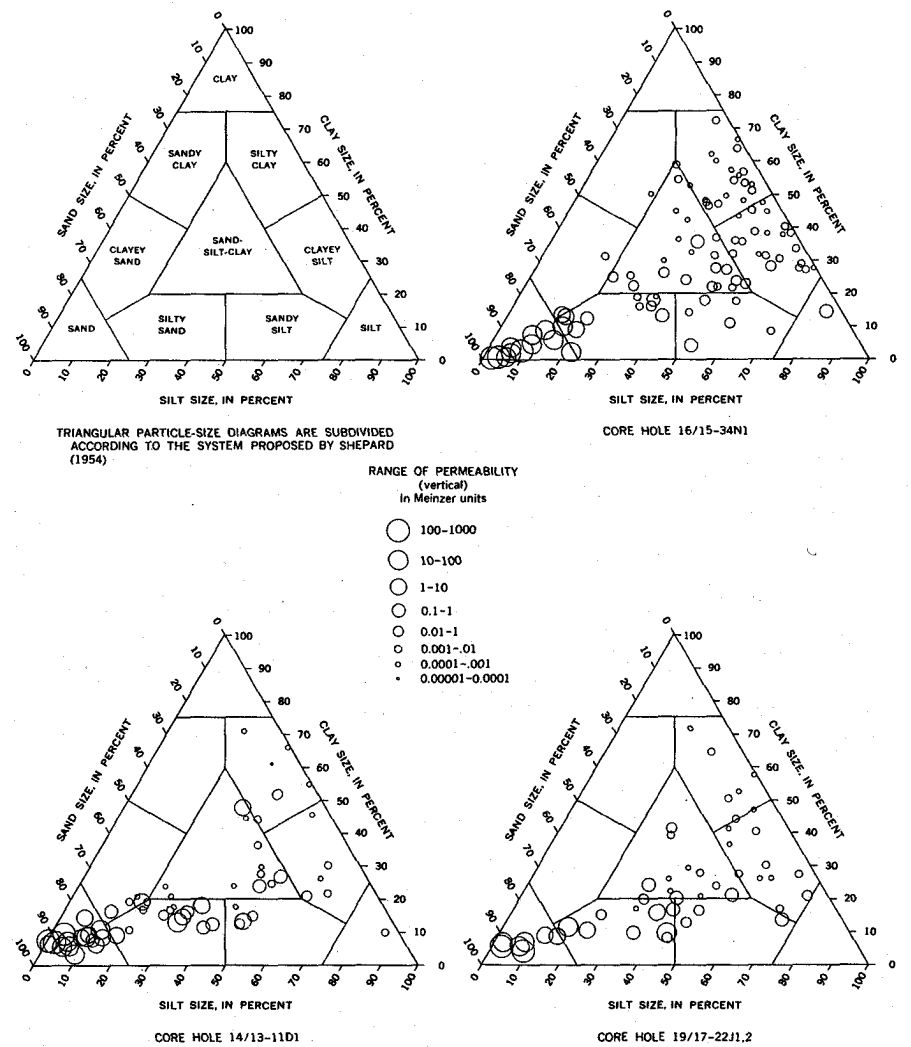


Figure 4.13 Relation between permeability and texture for samples from core holes in the Los Banos-Kettleman City area, California.

The log quartile deviation is the log of the geometrical quartile deviation, or sorting coefficient,  $S_0$ , and is represented by the equation

$$\text{Log } S_0 = (\log Q_3 - \log Q_1)/2 \quad (4.14)$$

The log  $S_0$  can be expressed to the base 10 (Krumbein and Pettijohn, 1938, p. 232) and is so tabulated in this report.

As noted by Krumbein and Pettijohn (1938, p. 232), the geometric quartile measures are ratios between quartiles and thus have an advantage over the arithmetic quartile measures in that they eliminate both the size factor and the unit of measurement. They do not, however, give a direct comparison because the log  $S_0$  (the log quartile deviation) increases arithmetically. Thus, a sediment having log  $S_0 = 0.402$  is twice as widely spread between  $Q_1$  and  $Q_3$  as one having log  $S_0 = 0.201$ .

Many sedimentologists now use a  $\emptyset$  scale in which

$$\emptyset = -\log_2 d, \quad (4.15)$$

in which  $d$  is the diameter of the particle in millimetres. This scale has certain advantages over the  $\log_{10}$  scale for expressing quartile deviation and other statistical parameters (Krumbein and Pettijohn, 1938, p. 233-235). Therefore, statistical parameters were listed in terms of the  $\emptyset$  scale in the report by Meade (1967) on the petrology of sediments in subsiding areas of central California.

#### 4.5.4 Permeability

The hydraulic conductivity depends in general on the degree of sorting and upon the arrangement and size of particles. It is usually low for clay and other fine-grained or tightly cemented materials and high for clean coarse gravel. In general, the hydraulic conductivity in a direction parallel to the bedding plane of the sediments (referred to in the data tables as horizontal permeability) is greater than the permeability perpendicular to the bedding plane (referred to as vertical permeability in the tables in this chapter). Most water-bearing materials of any significance as sources of water to wells have hydraulic conductivities above  $5 \times 10^{-3}$  cm per sec.

For central California, the hydraulic conductivities (coefficients of permeability) were presented in tables similar to Table 4.4, and in graphical form such as in Figures 4.12 and 4.13. Figure 4.12 shows the relation of horizontal and vertical hydraulic conductivity for many paired samples. Horizontal hydraulic conductivity was as much as 200 times greater than vertical hydraulic conductivity, with an average ratio of horizontal to vertical permeability of about 3.

Figure 4.14 shows the relation between vertical hydraulic conductivity and texture for samples from core holes in central California. Hydraulic conductivities have been grouped into eight ranges; a symbol representing the proper range for each sample is plotted in the appropriate textural location on the triangle, which is subdivided according to the system proposed by Shepard (1954). Although the highest hydraulic conductivity naturally occurs in the coarse-textured and well-sorted samples, conductivities within each textural classification vary considerably.

The vertical hydraulic conductivities for the clayey sediments tested in the variable-head permeameter under no load (Table 4.1) in general appear to be in a considerably higher range than those in Table 4.4 (ft per yr  $\times 9.7 \times 10^{-7}$  = cm per sec) which were computed from the consolidation tests for samples of similar texture. There are at least three reasons for this difference:

1. The permeability of a clayey sediment decreases markedly with decrease in void ratio (or porosity). The hydraulic conductivities given in Table 4.4 (in feet per year) are computed from time-consolidation data derived from test loads ranging from 7 to 112 kg per  $\text{cm}^2$  and thus represent conditions of substantially reduced void ratios from those of the samples tested in an unloaded condition in the variable-head permeameter. For sample 23L-207 (Table 4.4), the computed coefficient of vertical hydraulic conductivity for the load range 7 to 14 kg per  $\text{cm}^2$  is about 50 times as high as that for the load range 56 to 112 kg per  $\text{cm}^2$ .
2. For a clayey sediment, the water used for testing permeability in the variable-head permeameter, if not chemically compatible with the pore water, may affect the

results substantially. In the water used in the Hydrologic Laboratory for the variable-head tests, calcium was the predominant cation; however, sodium is the predominant cation in the pore water of the sediments beneath the Corcoran Clay Member in the San Joaquin Valley area. The use of water in which the calcium ion is predominant in testing cores of such sediments would tend to increase the value of the hydraulic conductivity obtained in the variable-head tests. The consolidation test, however, did not involve the passage of water through the sample, only the squeezing out of native pore water.

3. For a sample of very low hydraulic conductivity tested under no load in a variable-head permeameter, the disturbed condition of the sample at and near the container wall creates a boundary region which may produce a zone of appreciably higher permeability than that of the undisturbed sample matrix. Tests in a consolidometer, however, create lateral pressure against the container walls and thus tend to reduce the permeability of the disturbed boundary region to approximately that of the sample matrix.

For these three reasons, the coefficients of permeability of the clayey sediments as derived from the unloaded variable-head permeameter tests (Table 4.1) are not directly comparable to those computed from the time-consolidation data (Table 4.4). Coefficients from the consolidation tests are considered more reliable for samples taken as deep as these, but, to be meaningful for field applications, the coefficients would have to be computed at the void ratio or porosity, existing under the overburden (effective) stress conditions in the field.

#### 4.5.5 Specific gravity, unit weight, and porosity

The specific gravity of a sediment is the average of the specific gravities of all the constituent mineral particles. The specific gravity of most clean sands is usually near 2.65, whereas that of clays ranges from 2.5 to 2.9. Organic matter in the sediment will lower its specific gravity.

The dry unit weight of a sediment is dependent upon the shape, arrangement, and mineral composition of the constituent particles, the degree of sorting, the amount of compaction, and the amount of cementation. Dry unit weights of unconsolidated sediments commonly range from 1.3 to 1.8 g per cm<sup>3</sup>.

Because porosity is calculated from the dry unit weight and specific gravity of the sediment, it is dependent upon the same factors. Most natural sands have porosities ranging from 25 to 50 per cent, and soft clays from 30 to 60 per cent. Compaction and cementation tend to reduce these values. In general, porosities decrease with depth below land surface, and dry unit weights increase with depth. Athy (1930) described just such a progressive compaction of sediments as the load of overlying material increased with deposition.

The general trends discussed previously are complicated by other factors which affect the unit weight and porosity of individual samples. These factors are (1) differences in particle sizes or in particle-size distribution, (2) differences in type of clay mineral, (3) exposure to atmosphere and pre-consolidation, such as by dessication, during their depositional history (4) differences in intergranular structure as originally deposited, and (5) change in volume and structure of the core during and subsequent to the sampling operations.

The first four factors are natural phenomena, whereas the last one, the change in volume and structure of the core during and subsequent to the sampling operation, is introduced by man in his disturbance of the natural state in order to procure the sample. The sediments cored in the holes of the San Joaquin Valley ranged in depth from 21 to 630 m below the land surface. The effective stress, or grain-to-grain load, of the overburden on these materials in place increased from about 3 to 70 kg per cm<sup>2</sup> in this depth range. While the core was being cut, additional load was placed on the material by the core barrel and drill pipe, especially near the outer edge of the core. As soon as the materials were encased in the core barrel, however, the effective stress of the overburden was removed and they expanded elastically. Thus, the change in volume (porosity and unit weight) from the natural to the laboratory condition is a function of several variables:

1. Compacting effect produced by displacement of the material by the cutting edge, the inside-wall friction, or by overdriving of the core barrel.
2. Expanding effect of removal of the effective stress of the overburden load at the time the core enters the barrel; the magnitude depends on the elasticity of the material and on the amount of the effective stress removed (increasing with depth).

3. Disturbing effects of mechanical rotation of core-barrel teeth and core catcher while cutting the core, removal of core from barrel, packing, shipping, unpacking, and processing.

The net effect of this sampling process is believed to be an expansion of the sediments as tested in the laboratory, thus providing values that are higher for porosity and lower for unit weight than exist in the natural state. On the basis of a study of the consolidation and rebound data, the laboratory-determined porosity of the fine-textured materials from the San Joaquin Valley was estimated to be as much as 2-3 per cent higher than the in-place field porosity (J. F. Poland, written commun., 1963).

#### 4.5.6 Atterberg limits and indices

The Atterberg limits and indices determined for selected fine-textured samples from the core holes are presented in Tables 4.2 and 4.3. Predominantly fine-textured samples to be tested were selected by visual inspection. Because the Atterberg limits describe properties of the fine part of a sample, presenting Atterberg limit data for samples which are predominantly coarse textured could be misleading. When the influence which the limits of consistency have on the behavior of a sample is being judged, the percentage of the sample tested must be considered. Table 4.2 includes a column which lists the per cent (by weight) of the total sample that passed a No. 40 sieve (0.42-mm openings) and was therefore the part of the sample tested for Atterberg limits.

Most of these Atterberg limits and indices are not directly applicable to the study of subsidence and compaction of sediments under increased effective overburden load, but they do furnish a rough comparative measure of the way in which fine-grained sediments respond to a decrease in moisture content as they pass from the liquid to the solid state. Because the values of these indices are related to texture, composition, clay content, and type of clay minerals present, they may be of qualitative use in comparing the fine-textured clayey deposits in different areas to each other and to fine-textured sediments in other areas for which Atterberg indices have been obtained but for which the clay content, the compression index ( $C_c$ ), and the type of clay minerals present are not known.

The liquid and plastic limits (moisture content, in per cent by weight) for samples from all core holes in the central California subsidence areas are plotted against percentage of clay-size particles in figure 4.14. As shown by the trend lines, both limits tend to increase with an increase in clay content, the liquid limit increasing at a greater rate than the plastic limit.

The trend lines shown in Figure 4.14 were plotted from equations derived by computer. The equations are of the form  $y = a + bx$ , in which  $y$  represents the moisture content ( $w$ ),  $x$  represents the clay content ( $C$ ), both in per cent, and  $a$  and  $b$  are constants. In Figure 4.14A the equation of the liquid-limit trend line is  $w_L = 13.5 + 1.3C$  and that of the plastic-limit trend line is  $w_p = 17.3 + 0.54C$ . In Figure 4.14C the equation of the liquid-limit trend line is  $w_L = 14.0 + 0.72C$  and that of the plastic-limit trend line is  $w_p = 14.7 + 0.22C$ . The equations of all these trend lines are for samples having clay content based on the percentage of particles less than 0.004 mm in size.

Figure 4.14D shows trends which are composites of all the samples shown in Figures 4.14A-C. The equation of line 1, the liquid-limit trend line for clay sizes less than 0.002 mm, is  $w_L = 27.8 + 0.71C$ . The equation of line 2, the liquid-limit trend line for clay sizes less than 0.004 mm, is  $w_L = 25.8 + 0.60C$ . The equation of line 3, the plastic-limit trend line for clay sizes less than 0.002 mm is  $w_p = 25.6 + 0.21C$ . The equation of line 4, the plastic-limit trend line for clay sizes less than 0.004 mm is  $w_p = 24.5 + 0.19C$ . Lines 1 and 3 are included to show the relation between liquid and plastic limits and per cent of clay-size particles if 0.002 mm is chosen as the upper limit of the clay-size range.

The value of the standard error for each trend line was obtained by computer. The pairs of dashed lines which parallel each trend line designate two standard errors on either side of the trend line. The probability is 19 to 1 that, for a given value of clay content (in per cent), the observed liquid limit or plastic limit will lie within the interval between the dashed lines.

The difference between the liquid and plastic limits, or the plasticity index, represents the range of moisture content within which a sediment mass will remain in the plastic state. The moisture content difference between the liquid-limit trend line and the plastic-limit trend line in each part of Figure 4.14 represents the average plasticity index for different clay contents.

Table 4.2 Atterberg limits and indices of samples from core holes.

Hydrologic Laboratory sample	Depth (feet)	Percent passing No. 40 sieve	Liquid limit	Plastic limit	Shrinkage limit	Plasticity index	Flow index	Toughness index	Shrinkage index	Shrinkage ratio	Volumetric shrinkage	Linear shrinkage
<b>Core hole 14/13-11D1</b>												
57CAL1	77.0- 77.5	100	28	27	19	1	6	0.2	8	1.7	15	4
2	110.5- 111.0	99	56	26		30	18	1.9				
4	191.5- 192.0	100	33	24	15	9	8	1.1	9	1.8	32	8
5	232.5- 233.0	100	44	29	12	15	6	2.5	17	2.0	64	15
6	314.0- 314.5	100	34	24	18	10	8	1.3	6	1.7	27	8
7	386.0- 386.5	100	64	40	13	24	19	1.3	27	1.9	99	20
8	432.0- 432.5	100	59	36	12	23	28	2.8	24	2.0	114	22
9	510.3- 510.8	97	65	40	9	43	27	2.4	30	1.9	139	25
10	594.0- 594.5	100	82	39	8	25	11	2.3	32	2.0	114	22
12	646.6- 647.1	100	78	38	17	43	22	2.0	30	1.8	139	25
14	662.1- 662.6	100	80	44	24	36	11	3.3	20	1.6	90	19
16	674.0- 674.5	100	78	46	28	32	9	3.6	18	1.4	70	16
18	697.0- 697.5	100	67	38	28	31	11	2.8	8	1.5	58	14
19	713.0- 713.5	100	52	33	31	19	9	2.1	2	1.4	29	8
21	731.0- 731.5	100	58	34	15	24	26	.9	19	1.8	77	17
23	743.0- 743.5	100	46	28	21	18	19	.9	7	1.6	40	11
25	757.0- 757.5	98	30		27		11			1.5	4	1
26	764.9- 765.4	65	38	30	26	8	6	1.3	4	1.6	19	5
27	791.0- 791.5	100	40	30	20	10	10	1.0	10	1.7	34	9
28	802.0- 802.5	100	34	26	24	8	13	.6	2	1.7	17	5
29	826.0- 826.5	100	65	43	20	22	14	1.6	23	1.7	77	17
30	851.5- 852.0	100	31	26	19	5	25	.2	7	1.7	20	6
31	850.0- 850.5	100	42	31	23	11	10	1.1	8	1.6	30	8
32	857.5- 858.0	100	76	39	13	47	42	1.1	16	1.9	120	23
33	901.0- 901.5	100	40	30	20	10	15	.9	4	1.7	27	7
34	932.0- 932.5	99	47	23	10	24	4	2.7	10	2.0	74	17
35	936.5- 937.0	100	33	29	20	9	7	2.2	9	1.9	43	6
36	951.0- 951.5	100	34	27	13	7	6	1.2	14	1.7	22	6
37	968.5- 969.0	100	41	33	17	8	8	.7	16	1.8	40	11
38	984.0- 984.5	100	59	29	10	30	15	2.0	19	2.0	98	20
39	1,000.5-1,001.0	100	40	24	12	16	8	2.0	12	1.9	53	14
40	1,005.1-1,005.6	100	50	29	11	21	14	1.5	18	2.0	78	17
41	1,020.8-1,021.3	100	36	31	17	5	7	.7	14	1.8	34	9
42	1,039.5-1,040.0	100	47	34	12	13	10	1.3	22	1.9	67	16
43	1,051.5-1,052.0	100	33	24	17	9	10	.9	7	1.8	29	8
44	1,070.8-1,071.3	100	30	21	16	9	11	.8	5	1.8	25	7
45	1,104.6-1,105.1	88	25	22	15	3	15	.2	7	1.8	18	5
46	1,133.0-1,133.5	100	36	24	16	12	10	1.2	8	1.8	36	10
47	1,242.0-1,242.5	100	51	36	25	15	26	.6	11	1.5	39	11
48	1,312.0-1,312.5	98	26	18	18	8	4	2.0	0	1.8	14	4
49	1,339.5-1,340.0	100	26	18	23	10	6	1.7	3	1.6	21	6
50	1,357.0-1,357.5	100	46	26	10	23	14	1.6	13	2.0	72	17
51	1,362.5-1,363.0	100	32	23	18	21	16	1.7	3	1.7	24	7
52	1,385.0-1,385.5	100	54	36	13	18	12	1.5	23	1.8	74	17
53	1,397.0-1,397.5	98	61	41	5	4	4	2.8	34	2.1	118	23
54	1,432.5-1,433.0	100	77	38	4	39	14	2.8	24	2.3	168	28
55	1,446.0-1,446.5	100	56	28	5	28	15	1.9	23	2.2	112	22
56	1,454.5-1,455.0	100	44	33	16	11	9	1.2	17	1.7	48	13
57	1,465.0-1,465.5	100	58	34	8	24	11	2.2	26	2.1	105	21
<b>Core hole 16/15-34N1</b>												
58CAL2	296.2- 296.7	98	38	30	13	8	11	0.7	17	1.9	48	13
3	352.4- 352.9	98	40	26	12	14	14	1.0	14	1.9	53	14
4	413.5- 413.9	100	44	30	13	14	11	1.3	17	1.9	59	15
5	454.2- 454.5	99	54	37	8	17	23	.7	29	2.0	92	20
6	509.5- 510.0	100	46	35	15	11	18	.6	20	1.8	56	14
7	532.4- 532.9	97	42	32	12	12	9	.9	22	1.9	57	14
8	552.8- 553.2	100	45	32	11	11	13	.8	21	1.9	65	16
9	563.7- 564.2	100	56	46	12	10	18	1.6	34	1.9	84	18
10	570.7- 571.2	100	70	58	9	12	15	.7	49	2.0	122	23
11	636.4- 636.9	99	61	62	20	9	9	.6	32	1.6	66	16
12	643.2- 643.7	99	31	25	22	6	19	.3	3	1.6	14	4
13	662.6- 663.1	96	32	26	12	6	12	.5	14	1.8	36	10
14	666.0- 666.5	100	55	43	15	7	15	.8	26	1.8	72	17
15	683.7- 684.2	100	36	30	19	6	6	.4	11	1.7	29	8
16	696.6- 697.1	100	59	42	12	17	8	2.1	30	1.8	85	18
17	701.9- 702.4	100	42	32	17	10	18	.6	15	1.7	43	11
18	713.4- 713.9	99	61	40	7	21	16	1.3	33	2.0	108	22
19	732.0- 732.6	100	39	28	18	11	12	.9	10	1.7	36	10
20	753.8- 754.3	100	41	30	14	11	11	.6	16	1.8	49	13
21	762.4- 762.9	100	46	33	7	13	14	.9	26	2.0	78	17
22	773.9- 773.8	100	30	26	19	4	10	.4	7	1.7	19	5
23	806.1- 806.6	100	55	40	12	15	15	1.0	28	1.8	77	17
24	822.1- 822.6	98	60	49	10	41	20	.9	39	1.9	95	20
25	827.8- 828.2	100	47	33	13	14	14	.7	20	1.8	61	15
26	837.7- 838.2	100	58	43	13	15	20	.9	29	1.8	79	18
27	860.1- 860.6	100	31	24	22	7	13	.5	7	1.6	14	4
28	866.7- 867.3	100	30	23	18	7	7	1.0	5	1.7	20	6
29	891.6- 892.1	100	53	41	11	12	12	.8	30	1.9	80	18
30	922.6- 923.1	100	46	35	13	11	11	.8	22	1.8	59	15
31	931.2- 931.7	100	35	28	15	7	12	.6	13	1.8	36	10
32	940.6- 941.1	100	46	36	9	10	8	1.2	27	2.0	74	17
33	946.3- 946.8	100	63	43	7	20	22	.9	36	2.0	112	22
34	963.7- 964.2	100	37	28	16	9	10	.6	12	1.8	38	10
35	971.5- 972.0	100	57	46	16	11	20	.6	30	1.7	70	16
36	980.6- 981.1	100	35	27	27		14			1.5	12	3
37	1,042.8-1,043.3	100	51	45	14	6	13	.5	31	1.8	67	16
38	1,189.5-1,190.0	100	47	34	16	13	24	.5	18	1.8	56	14
39	1,225.0-1,225.5	100	38	34	25	4	14	.3	9	1.6	21	6
40	1,238.1-1,238.6	100	47	36	17	11	16	.7	19	1.7	51	13
41	1,254.9-1,255.4	100	41	36	30	8	7	.7	6	1.4	15	4

Table 4.3 Visual classification, Atterberg limits, and specific gravities of samples tested for consolidation.

[Data from Earth Laboratory, U.S. Bureau of Reclamation, Denver, Colo.]

Earth Laboratory sample	Depth (feet)	Gradation (estimated)				Color (wet)	Soil classification and description	Unified Soil Classification symbol	Atterberg limits			Specific gravity of solids
		Maximum size (U.S. Standard sieve No.)	Gravel >4.76 mm (percent)	Sand, 4.76-0.074 mm (percent)	Silt and clay <0.074 mm (percent)				Liquid limit (percent)	Plastic limit (percent)	Plasticity index	
Core hole 12/12-16H1												
23L81	84.3- 84.6	30	0	10	90	Brown	Clay, containing some fine sand; medium plasticity; slight dilatancy; medium dry strength; no reaction to HCl; trace of gypsum.	CL	31	14	17	2.80
92	159.4- 159.8	100	0	10	90	do	Clay, containing some fine sand; medium to high plasticity; slow dilatancy; medium reaction to HCl.	CL-CH	50	19	31	2.74
93	230.8- 231.2	50	0	10	90	Tan to brown	Clay, lean; low plasticity; slight dilatancy; low dry strength; slight reaction to HCl.	CL	33	11	22	2.73
94	324.5- 324.9	100	0	20	80	Gray	Clay, containing fine sand; low plasticity; medium dilatancy; some micaceous material present; no reaction to HCl.	CL	29	19	10	2.68
95	374.0- 374.5	200	0	0	100	do	Clay, fat; high plasticity; no dilatancy; no reaction to HCl.	CH	54	23	31	2.73
96	425.0- 425.3	100	0	10	90	do	Clay, fat, containing fine sand lenses; high plasticity; no dilatancy; no reaction to HCl; moist, and firm.	CH	76	27	49	2.67
97	471.2- 471.5	100	0	5	95	do	Clay, fat; high plasticity; no dilatancy; lensed with fine sand.	CH	58	20	38	2.68
98	516.5- 516.9	50	0	75	25	Gray to black	Sand, fine, no plasticity; fast dilatancy; strong organic odor present; soft and loosely cemented.	SM				2.70
99	579.0- 579.3	100	0	35	65	Tan	Clay, silty containing fine sand; medium plasticity; slight dilatancy.	CL	32	14	18	2.69
100	625.0- 625.4	200	0	0	100	Gray	Clay, fat; high plasticity; no dilatancy; firm; numerous planes containing some silt.	CH	59	19	40	2.79
101	675.9- 676.2	50	0	45	55	do	Clay, silty containing fine sand, medium plasticity, slow dilatancy; clay on outer surface; sand in center, angular.	CL	45	14	31	2.72
102	722.0- 722.3	100	0	5	95	do	Clay, fat; high plasticity; no dilatancy, blocky structure; fractures contain silt.	CH	70	20	50	2.69
103	773.0- 773.4	50	0	60	40	Brown to gray	Sand, fine containing silt; no plasticity; fast dilatancy; lensed with clay and silt; medium cementation; no reaction to HCl.	SM				2.77
104	821.4- 821.8	50	0	55	45	Gray	Sand, fine containing silt; no plasticity; fast dilatancy; organic odor present; no reaction to HCl.	SM				2.74
105	877.4- 877.8	30	0	65	35	Brown	Sand, fine, uniform; no plasticity; fast dilatancy; free water present; no reaction to HCl.	SM				2.71
106	926.8- 927.2	50	0	20	80	Gray	Clay, silty; medium plasticity; slow dilatancy; no reaction to HCl; top of sample contained sand of No. 30 size; rest of sample was silt and clay lensed.	CL	47	32	15	2.72
107	972.0- 972.4	30	0	75	25	do	Sand, fine; no plasticity; fast dilatancy; slight binder.	SM				2.70
108	986.6- 989.0	50	0	40	60	Brown	Clay containing fine sand; medium plasticity, slow dilatancy; sample lensed with clay and fine sand.	CL	37	20	17	2.68

Laboratory tests for properties of sediments in subsiding areas

Casagrande (1948, P. 919) devised a chart on which the liquid limit is plotted against the plasticity index and used it for rough classification of soils. Points representing different samples from the same stratum or fine-grained deposit plot as a straight line that is roughly parallel to an "A" line, an empirical boundary between typically inorganic clays above and plastic organic soils below the line. The higher a sample plots on this chart at a given liquid limit, the greater its toughness and dry strength and the lower its permeability and rate of volume change. Figure 4.15 shows plasticity charts of the Casagrande type on which the data for all samples tested from the central California subsidence areas have been plotted.

#### 4.5.7 Consolidation

As one phase of the research on subsidence and compaction of aquifer systems in central California, laboratory consolidation tests were made on representative cores from eight core holes. The results of these consolidation tests were utilized in interpretive reports of the Geological Survey to compute compaction in the confined aquifer system in response to the known decline in artesian head. The method has been described by Miller (1961); it is a refinement of a technique outlined by Gibbs (1959, p. 4-5) based upon Terzaghi's (1943) theory of consolidation and the use of one-dimensional consolidation tests. The consolidation test results are summarized as in Table 4.4.

Consolidation-test curves representative of samples from various depths in one of the San Joaquin valley core holes are shown in Figure 4.16. The curves show, in general, that the Corcoran Clay Member has a greater unit consolidation potential than any of the other sediments. The compaction of the Corcoran Clay Member, however, has contributed very little to the total subsidence to date (Miller, 1961, p. B57) because, where the Corcoran is thick, water moves out very slowly, owing to the formation's low vertical permeability. Where the Corcoran is thin and more permeable, it forms only a small percentage of the water-bearing section. Consolidation curves for the Corcoran Clay Member are generally steep in the load range 14-70 kg per cm<sup>2</sup> and indicate that the clay is normally loaded and has not been precompressed. Therefore the clay has only partly completed its potential consolidation at the present time and at the present artesian pressure.

##### 4.5.7.1 Estimating the compression index

Terzaghi and Peck (1948, p. 66), in a continuation of work begun by Skempton (1944, p. 126), state that the compression indices for clays in a remolded state ( $C'_c$ ) increase consistently with increasing liquid limit ( $w_L$ ). Using data from approximately 30 samples selected at random from different parts of the world and representing both ordinary and extra-sensitive clays, Terzaghi and Peck (1948) state that the data on compression indices and liquid limits for these clays plot on a graph within  $\pm 30$  per cent of a line representing the equation

$$C'_c = 0.007 (w_L - 10 \text{ per cent}). \quad (4.16)$$

They state further that for an ordinary clay of medium or low sensitivity tested in the undisturbed state, the value of  $C_c$  corresponding to field consolidation is approximately equal to 1.30  $C'_c$ ; thus,

$$C_c = 0.009 (w_L - 10 \text{ per cent}). \quad (4.17)$$

Hence, these authors conclude that for normally loaded clays with low or moderate sensitivity the compression index,  $C_c$  can be estimated approximately from knowledge of the liquid limit and use of equation 4.17. However, Terzaghi and Peck do caution that this approximate method of computation may furnish merely a lower limiting value for the compression index of an extra-sensitive clay. Later papers by Nishida (1956), and Roberts and Darragh (1963), showed exceptions to the compression index-liquid limit relationships described by Terzaghi and Peck (1948) and indicated a wide scattering of data. Furthermore, they found no simple correlation between these factors for the sample data they studied.

Figure 4.17 shows the relationship between liquid limit and compression index for core samples from test holes in subsiding areas of central California. Although the liquid limit is calculated as moisture content in per cent of dry weight, values usually are reported as numbers only and are reported thus in Figure 4.17 and henceforth in this section. The compression indices used in these graphs were obtained from consolidation tests, not by calculation from the

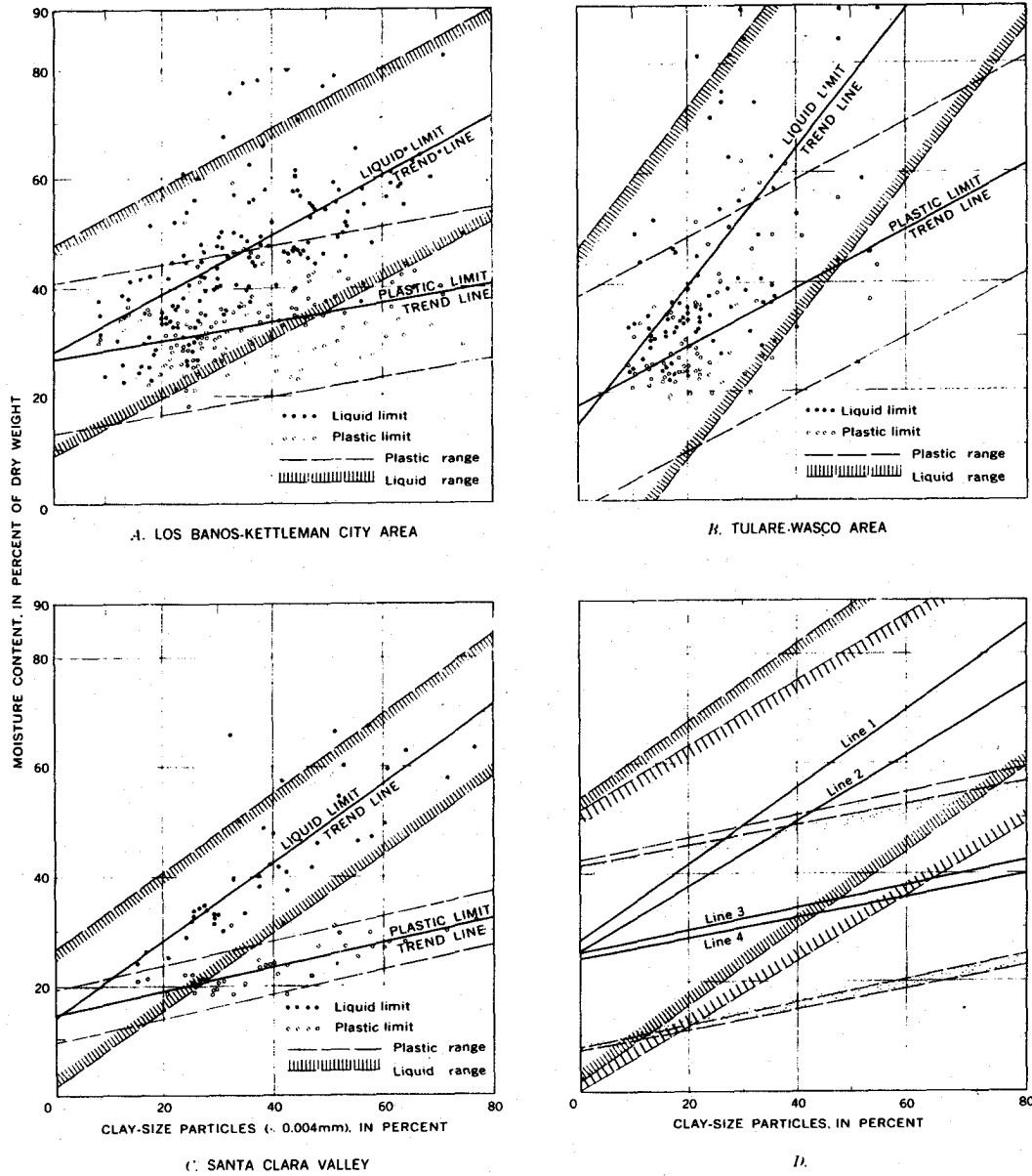


Figure 4.14 Effect of clay content on liquid limit; D, composite of all samples tested.

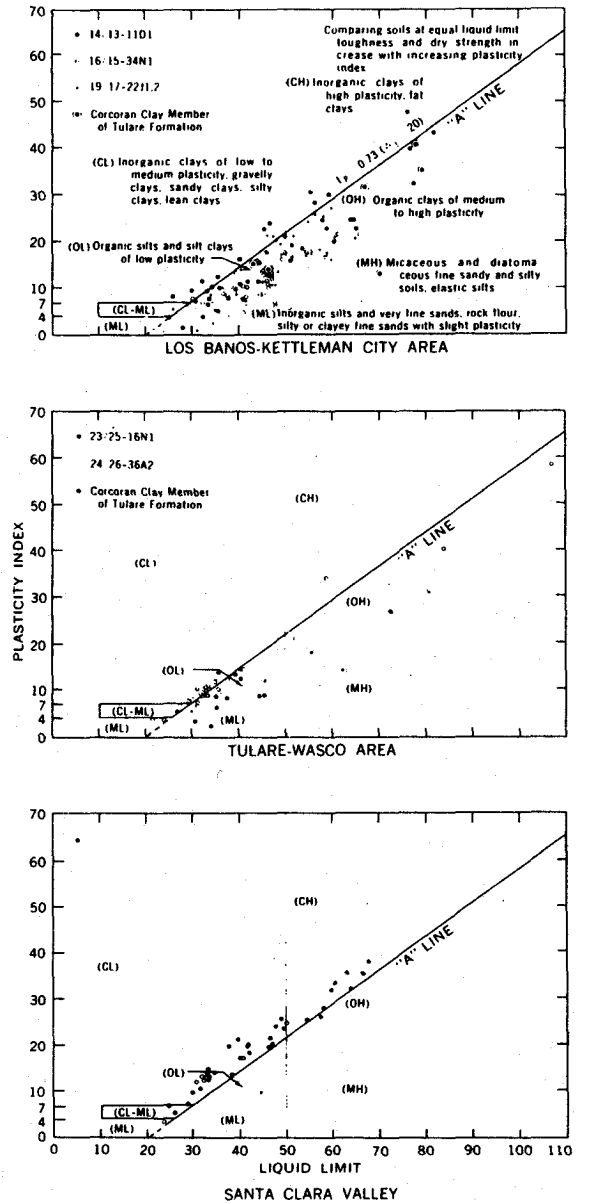


Figure 4.15 Unified soil classification for core-hole samples (ASTM, 1980).

Table 4.4 Consolidation test summaries.

[Data from Earth Laboratory, U.S. Bureau of Reclamation, Denver, Colo.]

Earth laboratory sample	Depth (feet)	Compression index, $C_c$		Time-consolidation data				Unified soil classification symbol	
		From consolidation curve	From Atterberg test	Load range (psi)	Coefficient of consolidation, $C_v$		Coefficient of permeability		
					Sq in. per sec	Sq ft per yr	Calculated (ft per yr)		From test (ft per yr)
<b>Core hole 12/12-16H1</b>									
23L91	84.3- 84.6	0.12	0.19	100- 200	$3.3 \times 10^{-4}$	72.5	$8.5 \times 10^{-3}$	CL	
92	159.4- 159.8	.22	.36	200- 400	$1.5 \times 10^{-4}$	31.8	$2.0 \times 10^{-3}$	CL-CH	
93	230.8- 231.2	.21	.21	100- 200	$9.2 \times 10^{-5}$	20.1	$2.8 \times 10^{-3}$	CL	
94	324.5- 324.9	.11	.17	200- 400	$5.1 \times 10^{-5}$	11.2	$1.3 \times 10^{-3}$	CL	
95	374.0- 374.5	.32	.39	200- 400	$1.7 \times 10^{-4}$	37.2	$4.0 \times 10^{-3}$	CH	
96	425.0- 425.3	1.13	.59	400- 800	$1.0 \times 10^{-5}$	2.2	$1.5 \times 10^{-4}$	CH	
97	471.2- 471.5	.90	.43	200- 400	$4.2 \times 10^{-5}$	0.92	$3.2 \times 10^{-4}$	CH	
98	516.5- 516.9	.41		400- 800	$3.2 \times 10^{-5}$	.70	$1.2 \times 10^{-4}$	CH	
99	579.0- 579.3	.23	.20	200- 400	$1.3 \times 10^{-4}$	28.5	$8.0 \times 10^{-3}$	SM	
				400- 800	$1.3 \times 10^{-4}$	28.5	$3.6 \times 10^{-3}$	CL	
100	625.0- 625.4	.34	.44	200- 400	$5.6 \times 10^{-5}$	122.0	$7.2 \times 10^{-3}$	CH	
101	675.9- 676.2	.27	.32	400- 800	$3.8 \times 10^{-5}$	83.2	$4.4 \times 10^{-3}$	CL	
102	722.0- 722.3	.34	.54	800-1,600	$2.5 \times 10^{-4}$	64.8	$1.5 \times 10^{-3}$	CH	
103	773.0- 773.4	.33		400- 800	$1.7 \times 10^{-5}$	3.7	$2.6 \times 10^{-4}$	CH	
104	821.4- 821.8	.20		800-1,600	$8.0 \times 10^{-5}$	1.8	$6.0 \times 10^{-5}$	CL	
105	877.4- 877.8	.18		400- 800	$1.1 \times 10^{-3}$	232.1	$1.2 \times 10^{-2}$	CH	
106	926.8- 927.2	.68	.34	800-1,600	$6.9 \times 10^{-4}$	151.1	$4.8 \times 10^{-3}$	SM	
107	972.0- 972.4	.33		400- 800	$2.7 \times 10^{-5}$	5.9	$3.3 \times 10^{-4}$	SM	
108	998.6- 999.0	.30	.24	800-1,600	$6.0 \times 10^{-5}$	1.3	$5.0 \times 10^{-5}$	CL	
				400- 800	$1.6 \times 10^{-4}$	35.0	$3.7 \times 10^{-3}$	SM	
				800-1,600	$8.5 \times 10^{-5}$	18.6	$1.2 \times 10^{-3}$	CL	
							14.2	SM	
							33.9	SM	
							38.4	SM	
							1.4	CL	
<b>Core hole 14/13-11D1</b>									
23L80	315.0- 315.3			200- 400	$1.8 \times 10^{-4}$	39.4	$4.0 \times 10^{-3}$	SP	
194	397.0- 397.3	0.36		400- 800	$5.1 \times 10^{-5}$	11.2	$8.1 \times 10^{-4}$	CL	
81	554.0- 554.4	.22		800-1,600	$1.2 \times 10^{-5}$	2.6	$9.0 \times 10^{-5}$	CL	
83	699.0- 699.4	.97		200- 400	$6.8 \times 10^{-5}$	15.0	$9.5 \times 10^{-4}$	CL	
84	746.0- 746.4	.30		400- 800	$2.2 \times 10^{-5}$	4.9	$2.2 \times 10^{-4}$	CL	
196	832.2- 832.7	.36		800-1,600	$4.1 \times 10^{-5}$	9.0	$1.8 \times 10^{-4}$	CL	
85	983.6- 984.0	0.35		400- 800	$5.8 \times 10^{-5}$	12.8	$2.1 \times 10^{-4}$	CL	
86	1,076.0-1,076.4			800-1,600	$3.2 \times 10^{-5}$	7.1	$5.0 \times 10^{-4}$	CL	
88	1,350.5-1,350.8			200- 400	$1.7 \times 10^{-4}$	37.4	$2.6 \times 10^{-3}$	CL	
89	1,395.0-1,395.3			400- 800	$1.2 \times 10^{-4}$	26.9	$1.5 \times 10^{-3}$	CL	
90	1,450.0-1,450.3	.29		800-1,600	$6.6 \times 10^{-5}$	14.5	$5.5 \times 10^{-4}$	CL	
				200- 400	$2.0 \times 10^{-4}$	43.8	$3.6 \times 10^{-3}$	CL	
				400- 800	$6.7 \times 10^{-5}$	14.7	$9.4 \times 10^{-4}$	CL	
				800-1,600	$4.5 \times 10^{-5}$	9.9	$3.7 \times 10^{-4}$	CL	
				200- 400	$1.2 \times 10^{-5}$	2.6	$2.1 \times 10^{-4}$	CL	
				400- 800	$1.0 \times 10^{-5}$	2.2	$1.1 \times 10^{-4}$	CL	
				800-1,600	$1.2 \times 10^{-5}$	2.6	$1.2 \times 10^{-4}$	CL	
							1.7	SM	
							19.3	SP	
				200- 400	$1.0 \times 10^{-4}$	21.8	$1.2 \times 10^{-3}$	CL	
				400- 800	$1.7 \times 10^{-5}$	3.6	$1.5 \times 10^{-4}$	CL	
				800-1,600	$1.1 \times 10^{-5}$	2.4	$8.0 \times 10^{-5}$	CL	
				800-1,600	$3.9 \times 10^{-5}$	8.4	$2.4 \times 10^{-4}$	CL	
<b>Core hole 16/15-34N1</b>									
23L197	299.1- 299.5	0.34	0.38	200- 400	$3.4 \times 10^{-4}$	74.9	$1.1 \times 10^{-2}$	CH	
198	418.1- 418.5	.32	.31	100- 200	$1.7 \times 10^{-3}$	361.4	$6.3 \times 10^{-2}$	CL	
200	538.9- 539.2	.30	.42	200- 400	$5.0 \times 10^{-4}$	109.5	$1.3 \times 10^{-2}$	CH	
201	571.2- 571.6	.65	.65	400- 800	$1.4 \times 10^{-4}$	30.7	$2.1 \times 10^{-3}$	CH	
202	636.9- 637.3	.70	.63	200- 400	$3.4 \times 10^{-4}$	74.5	$6.3 \times 10^{-3}$	CH	
204	713.1- 713.4	.31	.46	400- 800	$1.3 \times 10^{-4}$	28.5	$2.1 \times 10^{-3}$	CH	
206	859.7- 860.1	.19	.19	800-1,600	$5.6 \times 10^{-4}$	122.8	$4.6 \times 10^{-3}$	SC	
207	901.7- 902.1	.29	.55	100- 200	$1.4 \times 10^{-4}$	30.7	$3.0 \times 10^{-3}$	CH	
				200- 400	$3.1 \times 10^{-5}$	6.6	$4.9 \times 10^{-4}$	CH	
				400- 800	$1.6 \times 10^{-5}$	3.5	$2.0 \times 10^{-4}$	CH	
				800-1,600	$7.5 \times 10^{-6}$	1.6	$6.1 \times 10^{-5}$	CH	
208	972.0- 972.4	.42	.53	200- 400	$2.3 \times 10^{-4}$	60.4	$3.1 \times 10^{-3}$	CH	
				400- 800	$2.2 \times 10^{-5}$	4.8	$3.6 \times 10^{-4}$	CH	
				800-1,600	$6.5 \times 10^{-6}$	1.4	$7.0 \times 10^{-5}$	CH	
210	1,153.6-1,154.0	.21	.23	400- 800	$6.2 \times 10^{-4}$	135.8	$5.1 \times 10^{-3}$	CL	
				800-1,600	$3.2 \times 10^{-5}$	70.0	$2.2 \times 10^{-3}$	CL	
212	1,237.7-1,238.1			400- 800	$3.7 \times 10^{-5}$	8.1	$2.7 \times 10^{-4}$	CH	

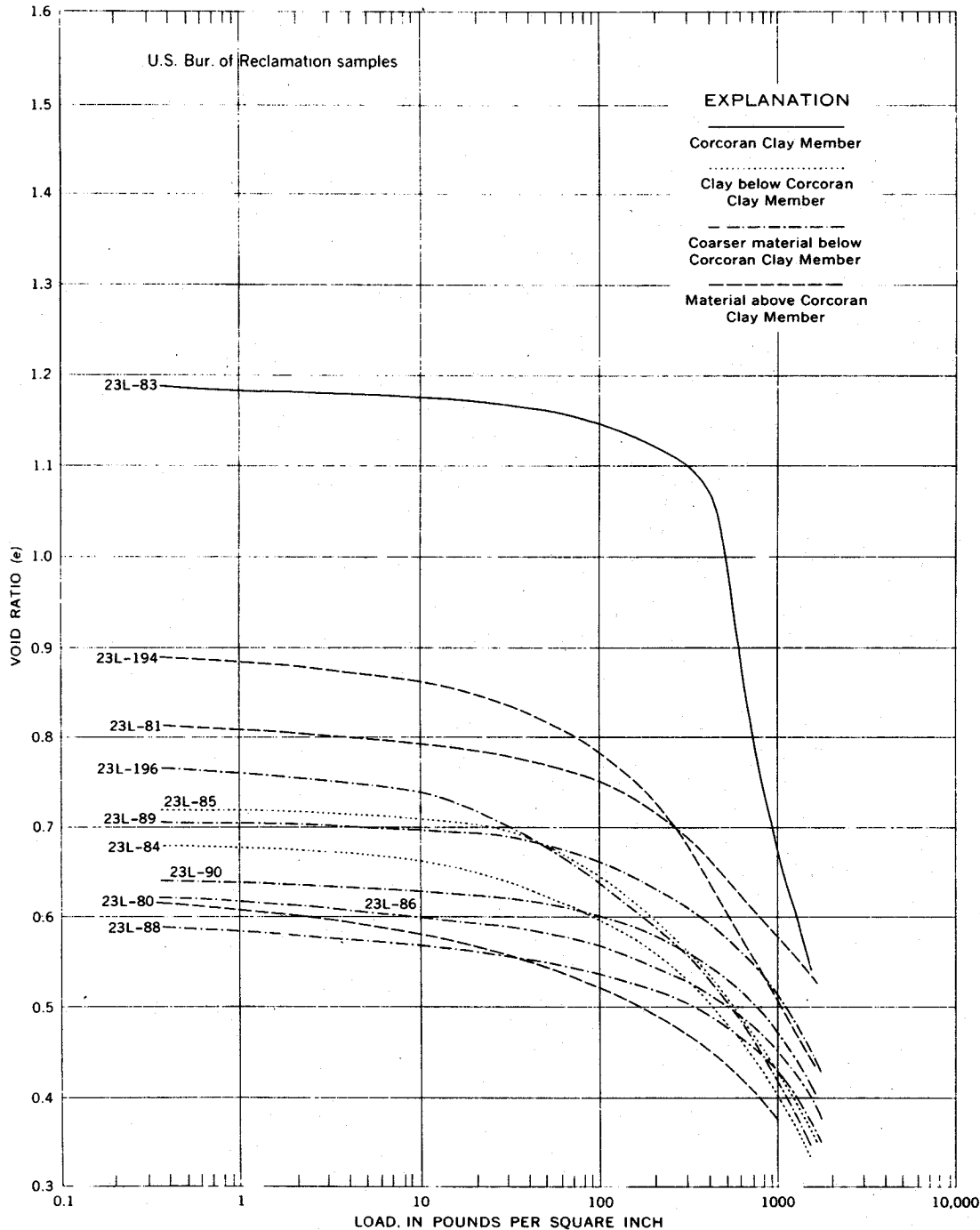


Figure 4.16 Void ratio/load curves for selected samples from core hole 14/13-11D1 in the San Joaquin Valley, California.

Terzaghi and Peck equation. The solid line in each of the parts of Figure 4.17 represents the regression line for the Terzaghi and Peck equation,  $C_c = 0.0009 (w_L - 10)$ .

The data in Figure 4.17 show that 10 of the 22 samples from the Los Banos-Kettleman City area, 11 of the 12 samples from the Tulare-Wasco area, and 4 of the 21 samples, from the Santa Clara Valley, lie outside the  $\pm 30$  per-cent limits of scatter about the regression line for the Terzaghi and Peck equation,  $C_c = 0.0009 (w_L - 10)$ . Three samples of clay in the Los Banos-

Kettleman City area have compression indices approximately twice as large as would be predicted from the Terzaghi-Peck equation. The void ratio-load curves for these three samples suggest that they are extrasensitive clays and, if so, they would be expected to plot well above the equation line. However, even if these samples are excluded, the data of Figure 4.17 show that the relationship between liquid limit and compression index for fine-textured sediments on the west side of the San Joaquin Valley does not fit the Terzaghi-Peck equation as closely as might be expected from the discussion by those authors (Terzaghi and Peck, 1948), p. 66).

Regression lines were determined by computer for the liquid limit-compression index relationship for samples from core holes in the San Joaquin and Santa Clara Valleys. Table 4.5 presents the equations of the regression lines for data from the central California area so they can be compared with the regression line for the Terzaghi and Peck equations,  $C'_c = 0.0007 (w_L - 10)$  and  $C_c = 0.0009 (w_L - 10)$ . The table shows that only the equation for core hole 16/15-34N1 is approximately equivalent to either equation discussed by Terzaghi and Peck. Figure 4.17, part D, and Table 4.5 show that the equation of the regression line for 11 samples from the San Joaquin Valley (except the three samples with the exceptionally high compression indices) is  $C_c = 0.014 (w_L - 22)$  and the equation for the Santa Clara Valley is  $C_c = 0.003 (w_L + 35)$ .

#### 4.5.7.2 Correlation of compression indices

Figure 4.18 demonstrates the correlation between compression indices estimated from liquid-limit tests and those determined from consolidation curves such as are shown in Figure 4.16. In Figure 4.18 the heavy line passing through the origin at an angle of 45 degrees to the x and y axes represents absolute correlation between the values represented by the two axes. The compression indices estimated from liquid limits for the Los Banos-Kettleman City area and Santa Clara Valley generally are higher than those determined from consolidation curves and those for the Tulare-Wasco area are lower.

The data in Figure 4.18 also show that the sediments of marine origin have much higher compression indices when determined from consolidation curves than when estimated from liquid limits. Furthermore, sediments of lacustrine origin have somewhat lower compression indices when determined from consolidation curves than when estimated from liquid limits. Again, the explanation may be due to the difference in load conditions, the marine sediments being the deepest and the alluvial sediments being the shallowest.

#### 4.5.7.3 Estimating coefficients of consolidation

Figure 4.19 shows the computed coefficient of consolidation for 1 to 4 different load ranges plotted against liquid limit for samples from the central California areas. Although the coefficient of consolidation shows a general decrease for increasing values of liquid limit, Figure 4.17 indicates that the coefficient of consolidation for any particular load range can vary through more than one order of magnitude for any given liquid limit. Terzaghi and Peck (1948, pp. 76-77) described a similar relationship for data from about 30 samples and noted that the relationship is different for each core hole as well as for each area.

#### 4.5.7.4 Effect of soil classification

Information in Figures 4.17 and 4.18 indicates the effect of particle size and texture on the consolidation characteristics and the liquid limit. The Unified Soil Classification (Am. Soc. Testing Materials, 1964, pp. 208-220) designation, which is based on texture, is indicated at the top of Figure 4.17.

In general, those samples with a classification of CH-MH have the largest liquid limits and compression indices, and the smallest coefficients of consolidation. Samples with a classification of SC and SM have the smallest liquid limits and compression indices, and the largest coefficient of consolidation. Samples with a classification of ML, CL and CH have values somewhere between these two extremes. Samples of sediments of alluvial origin tended to be classified as CL and CH; and those of marine origin were classified primarily as CH-MH.

#### 4.5.7.5 Relationship of consolidation characteristics and liquid limits

Data presented in this chapter show that the equations presented by Terzaghi and Peck (1948) (equations 4.16 and 4.17) do not apply to the relationship between compression index and liquid limit for sedimentary deposits tested from the central California subsidence areas.

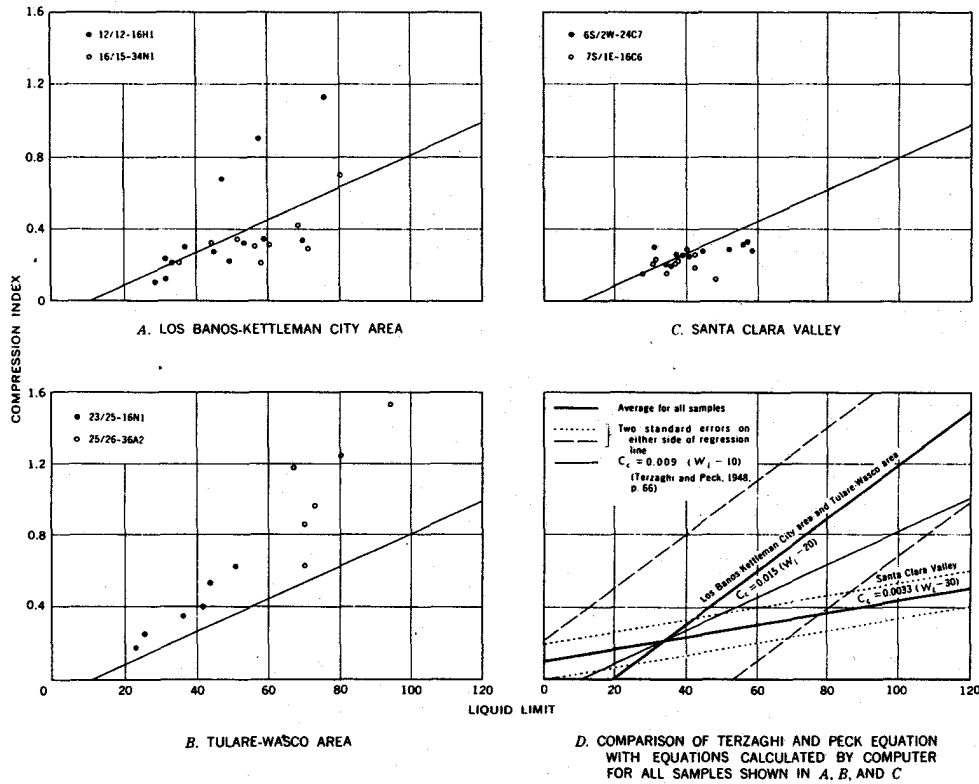


Figure 4.17 Relation between liquid limit and compression index for selected samples from core holes in San Joaquin and Santa Clara Valleys, California.

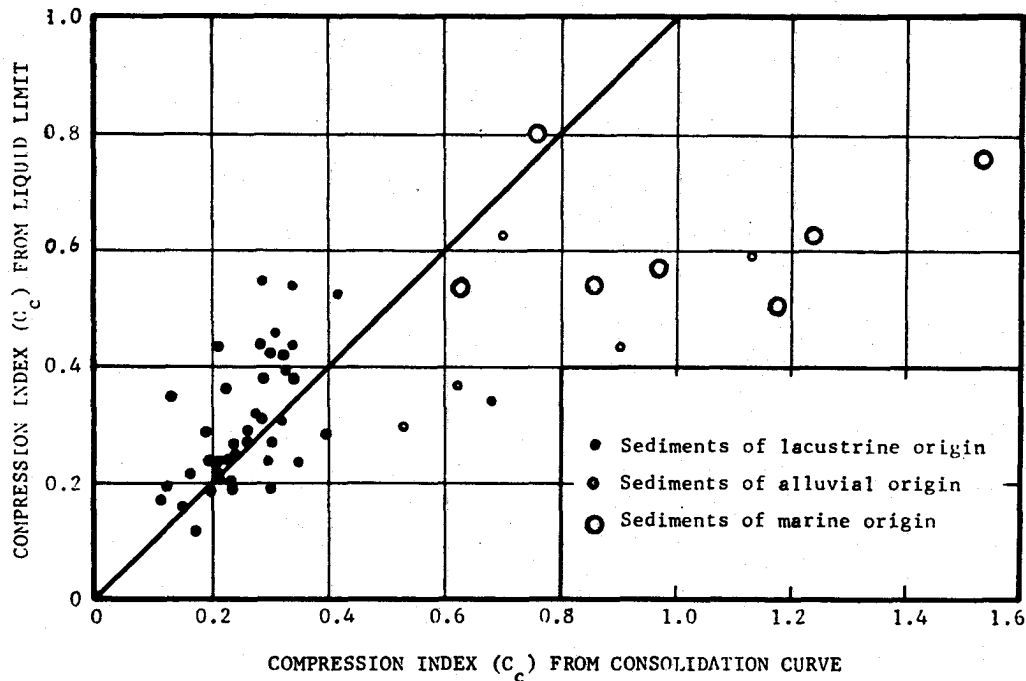


Figure 4.18 Comparison of two methods for determination of compression index for all samples from subsidence areas in the San Joaquin and Santa Clara Valleys, California.

Table 4.5 Equations for regression lines for various groups of data from subsiding areas in central California

Data used	Equation
Los Banos-Kettleman City area	
Core hole 12/12-16H1, exclusive of the 3 samples with exceptionally high compression indices	$C_C = 0.005 (w_L - 6)$
Core hole 16/15-34N1	$C_C = 0.007 (w_L - 12)$
All samples in area, exclusive of 3 samples with exceptionally high compression indices	$C_C = 0.006 (w_L - 3)$
Tulare-Wasco area	
Core hole 23/25-16N1	$C_C = 0.015 (w_L - 1)$
Core hole 24/26-36A2	$C_C = 0.024 (w_L - 32)$
All samples in area	$C_C = 0.018 (w_L - 16)$
San Joaquin Valley, exclusive of 3 samples with exceptionally high compression indices	$C_C = 0.014 (w_L - 22)$
Santa Clara Valley	
Core hole 6S/2W-24C7	$C_C = 0.003 (w_L - 47)$
Core hole 7S/1E-16C6	$C_C = 0.0005 (w_L + 370)$
All samples in area	$C_C = 0.003 (w_L + 35)$

Furthermore, the data show that no single equation applies to the relationship for all areas studied, with the following equations being obtained for the two valleys:

$$\text{San Joaquin Valley: } C_C = 0.014 (w_L - 22); \quad (4.18)$$

$$\text{Santa Clara Valley: } C_C = 0.003 (w_L + 35). \quad (4.19)$$

In essentially every case, the equations of the regression lines represent only general trends because there is considerable scatter of data for all core holes. The trend line for data from the Santa Clara Valley is so nearly horizontal that a rather narrow range of compression indices could be obtained over a wide range of liquid limits. Compression indices estimated from liquid limits, however, showed better correlation with indices determined from consolidation curves when the sediments were of alluvial or lacustrine origin than when they were of marine origin.

All coefficients of consolidation showed a general decrease for increasing values of liquid limit. However, because the coefficients for any particular load range could vary through more than one order of magnitude for any given liquid limit, the relationship could not be estimated with reasonable accuracy. In fact, the general trend for the relationship even varies, for each subsidence area and for each core hole.

At least for the areas studied in central California, the consolidation characteristics of the undisturbed sediments in the field cannot be closely approximated by liquid limits, which are made on disturbed samples of those sediments. The studies also indicate that the equations reported by Terzaghi and Peck (1948) must be used with extreme caution to estimate the consolidation characteristics of sediments in areas of subsidence--especially if the compacting sediments are at considerable depth.

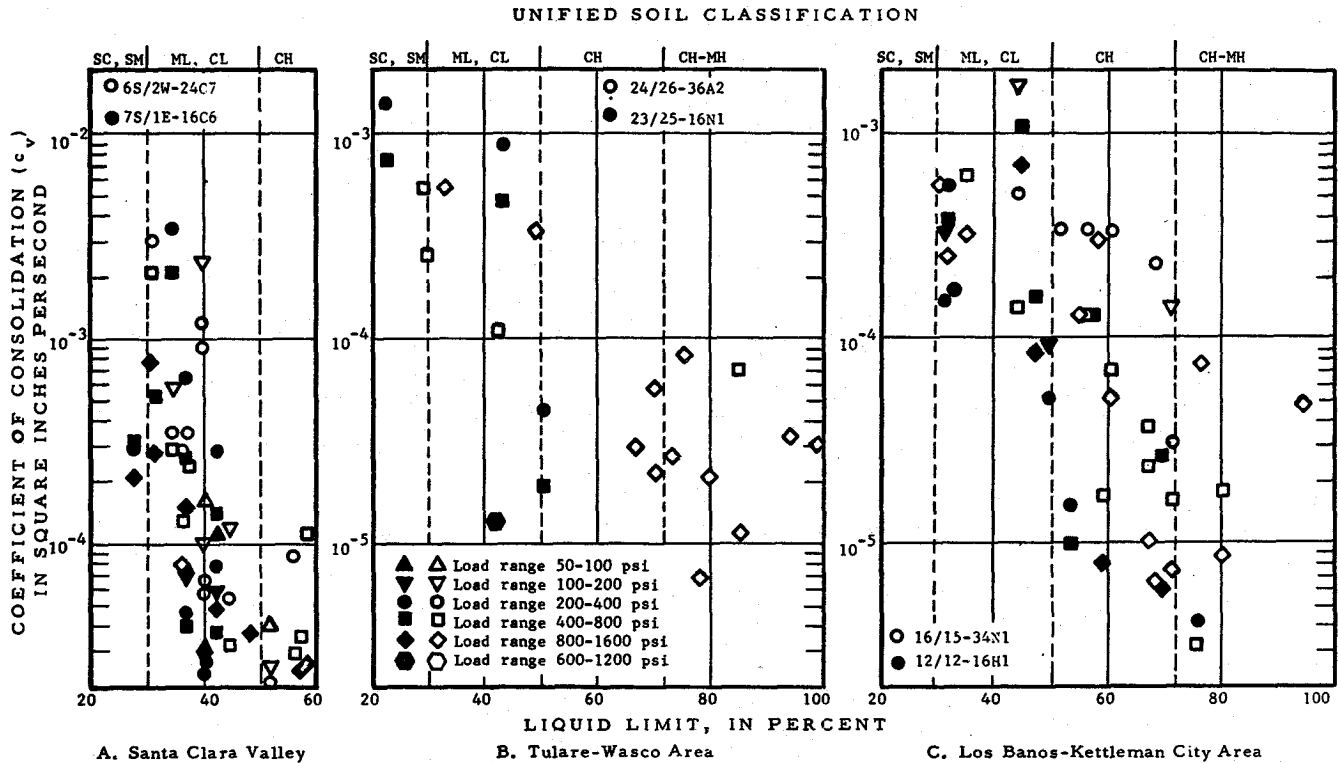


Figure 4.19 Relation of coefficient of consolidation to liquid limit for samples from core holes in the San Joaquin and Santa Clara Valleys, California.

4.6 REFERENCES

AMERICAN GEOLOGICAL INSTITUTE. 1960. Glossary of geology and related sciences, 2d ed. Washington, 397 p.

AMERICAN SOCIETY FOR TESTING MATERIALS. 1980. Annual Book of Standards, Part 19. Philadelphia, 654 p.

ATHY, L. P. 1930. Density, porosity, and compaction of sedimentary rocks. Am. Assoc. Petroleum Geologists Bull., v. 14, pt. 1, no. 1, p. 1-24.

ATTERBERG, A. 1911. Über die physikalische bodenuntersuchung, und Über die plastizität der tone. Internat. Mitt. Bodenkunde, v. 1, p. 10-43.

BULL, W. B. 1961. Causes and mechanics of near-surface subsidence in western Fresno County, California, in Short papers in the geologic and hydrologic sciences. U.S. Geol. Survey Prof. Paper 424-B, p. B187-B189.

BULL, W. B. 1964. Alluvial fans and near-surface subsidence, western Fresno County, California. U.S. Geol. Survey Prof. Paper 437-A, p. A1-A71.

CALIFORNIA STATE WATER RESOURCES BOARD. 1955. Santa Clara Valley investigation, Sacramento, Bull., 7, 154 p.

- CASAGRANDE, ARTHUR. 1932. Research on the Atterberg limits of soils. *Public Roads*, v. 13, no. 9, p. 121-136.
- CASAGRANDE, ARTHUR. 1948. Classification and identification of soils. *Am. Soc. Civil Engineers Trans.*, v. 113, p. 901-930.
- CLARK, W. O. 1924. Ground water in Santa Clara Valley, California. U.S. Geol. Survey Water Supply Paper 519, 209 p.
- DAVIS, G. H., and POLAND, J. F. 1957. Ground-water conditions in the Mendota-Huron are Fresno and Kings Counties, California. U.S. Geol. Survey water-Supply Paper 1360-G, 409-588.
- GIBBS, H. J. 1953. Estimating foundation settlements by one-dimensional consolidation test Denver, Colo. U.S. Bureau of Reclamation Eng. Mon. 13, 24 p.
- GIBBS, H. J. 1959. A laboratory testing study of land subsidence. Pan-Am. Conf. Soil Mech Found. Eng., 1st, Mexico City, 1959, Proc., p. 3-36.
- GOLDSCHMIDT, V. M. 1926. Undersokelser over lersedimenter. Beretning om Nordiske Jordbrugs forskeres Kongress i Osla, Copenhagen Nordisk Jordsbrugsforskning, v. 4, no. 7, p. 434-445.
- INTER-AGENCY COMMITTEE ON LAND SUBSIDENCE IN THE SAN JOAQUIN VALLEY. 1955. Proposed program for investigating land subsidence in the San Joaquin Valley, California. Sacramento, Calif., 60 p.
- INTER-AGENCY COMMITTEE ON LAND SUBSIDENCE IN THE SAN JOAQUIN VALLEY. 1958, Progress report on land-subsidence investigations in the San Joaquin Valley, California, through 1957. Sacramento, Calif., 160 p. 45 pls., 5 tables.
- JOHNSON, A. I., and MORRIS, D. A. 1962a. Physical and hydrologic properties of water-bearing deposits from core holes in the Los Banos-Kettleman City area, California. U. S. Geological Survey open file report, 182 p.
- JOHNSON, A. I., and MORRIS, D. A. 1962b. Relation of volumetric shrinkage to clay. content of sediments from the San Joaquin Valley, California, in Short papers in geology, hydrology, an topography. U.S. Geol. Survey Prof. Paper 450-B, p. B43-B44.
- JOHNSON, A. I., and MOSTON, R. P. 1969. Relationship of consolidation characteristics an Atterberg limits for subsiding sediments in Central California, U.S.A. Internat. Symposium on Land Subsidence, Tokyo, IAHS, p. 579-587.
- JOHNSON, A. I., MOSTON, R. P., and MORRIS, D. A. 1968. Physical and hydrologic properties of water-bearing deposits in subsiding areas in central California. U.S. Geol. Survey Prof. Paper 497-A, 71 p., 14 pls.
- KRUMBEIN, W. C., and PETTIJOHN, F. J. 1938. Manual of sedimentary petrography. New York, Appleton-Century-Crofts, Inc., 549 p.
- LANE, E. W., Chairman. 1947. Report of the Subcommittee on Sediment Terminology. *Am. Geophys. Union Trans.*, v. 28, p. 936-938.
- LOFGREN, B. E. 1960. Near-surface land subsidence in western San Joaquin Valley, California. *Jour. Geophys. Research*, v. 65, no. 3, p. 1053-1062.
- LOFGREN, B. E. 1963. Land subsidence in the Arvin-Maricopa area, San Joaquin Valley, California, in Short papers in geology and hydrology. U.S. Geol. Survey Prof. Paper 475-B, p. B171-175.
- LOFGREN, B. E. 1969. Field measurement of aquifer-system compaction, San Joaquin Valley, California. Internat. Symposium on Land Subsidence, Tokyo--1969, I.A.S.H. Pub. 88, p. 272-284.

- MEADE, R. H. 1964. Removal of water and rearrangement of particles during the compaction of clayey sediments--review. U.S. Geol. Survey Prof. Paper 497-B. 23 p.
- MEADE, R. H. 1967. Petrology of sediments underlying areas of land subsidence in central California. U.S. Geol. Survey Prof. Paper 497-C, 83 p.
- MEINZER, O. E. 1923. The occurrence of ground water in the United States, with a discussion of principles. U.S. Geol. Survey Water-Supply Paper 489, 321 p.
- MEINZER, O. E., ed. 1949. Hydrology, in Physics of the Earth. New York, Dover Pubs., Inc., 712 p.
- MILLER, R. E. 1961. Compaction of an aquifer system computed from consolidation tests and decline in artesian head, in Short papers in the geologic and hydrologic sciences. U.S. Geol. Survey Prof. Paper 424-B, p. B54-58.
- MORRIS, D. A., and JOHNSON, A. I. 1959. Correlation of Atterberg limits with geology of deep cores from subsidence areas in California. Am. Soc. Testing Materials Spec. Tech. Pub. 254, p. 183-187.
- NISHIDA, YOSHICHIKA. 1956. A brief note on compression index of soil. Am. Soc. Civil Engineers, Soil Mech. Found. Div. Jour., vol. 82, SM 3, Paper 1027, 14 p.
- POLAND, J. P. 1960. Land subsidence in the San Joaquin Valley, California, and its effect on estimates of ground-water resources, in International Association of Scientific Hydrology Commission of Subterranean Waters. I.A.S.H. pub. 52, p. 324-335.
- POLAND, J. P. 1969. Land subsidence and aquifer system compaction, Santa Clara Valley, Calif. Internat. Symposium on Land Subsidence, Tokyo 1969, I.A.S.H. pub. 88, p. 285-294.
- POLAND, J. F., and DAVIS, G. H. 1956. Subsidence of the land surface in the Tulare-Wasco (Delano) and Los Banos-Kettleman City areas, San Joaquin Valley, California. Am. Geophys. Union Trans., v. 37, no. 3, p. 287-296.
- POLAND, J. F., and GREEN, J. H. 1962. Subsidence in the Santa Clara Valley, California--A progress report. U.S. Geol. Survey Water-Supply Paper 1619-C, 16 p.
- REITEMEIER, R. F. 1946. Effect of moisture content on the dissolved and exchangeable ions of soils of arid regions. Soil Sci., v. 61, p. 195-214.
- RILEY, F. S. 1969. Analysis of bore-hole extensometer data from Central California. Internat. Symposium on Land Subsidence, Tokyo 1969, I.A.S.H. pub. 89, p. 423-431.
- ROBERTS, D. V., and DARRAGH, R. D. 1962. Areal fill settlements and building foundation behavior at the San Francisco airport, in Field testing of soils. Am. Soc. Testing materials Spec. Tech. Pub. 322, p. 211-230.
- SHEPARD, F. P. 1954. Nomenclature based on sand-silt-clay ratios. Jour. Sed. Petrology, v. 24, no. 3, p. 151-158.
- SKEMPTON, A. W. 1944. Notes on the compressibility of clays. Geol. Soc.--London Quart. Jour., vol. C, p. 119-135.
- TAYLOR, D. W. 1948. Fundamentals of soil mechanics. New York, John Wiley & Sons, Inc., 700 p.
- TERZAGHI, KARL. 1926. Simplified soil tests for subgrades and their physical significance. Public Roads, v. 7, p. 153-162.
- TERZAGHI, KARL. 1943. Theoretical soil mechanics. New York, John Wiley & Sons, Inc., 510 p.
- TERZAGHI, KARL, and PECK, R. B. 1,948. Soil mechanics in engineering practice. New York, John Wiley & Sons, Inc. 566 p.

TRASK, P. D. .1932. Origin and environment of source sediments of petroleum, Houston. Gulf Publishing Co., 323 p.

TWENHOFEL, W. H., and TYLER, S. A. 1941. Methods of study of sediments. New York, McGraw-Hill Book Co., Inc., 183 p.

U.S. BUREAU OF RECLAMATION. 1974. Earth manual. Denver, 751 p.

WENTWORTH, C. K. 1922. A scale of grade and class terms for elastic sediments. Jour. Geology, v. 30, p. 377-392.

WENZEL, L. K. 1942. Methods for determining permeability of water-bearing materials. U.S Geol. Survey Water-Supply Paper 887, 192 p.